Recent Advancements in Multimodal Medical Image Fusion Techniques for Better Diagnosis: An overview

Send Orders for Reprints to reprints@benthamscience.net

Current Medical Imaging, XXXX, *XX*, 000-000

REVIEW ARTICLE

Recent Advancements in Multimodal Medical Image Fusion Techniques for Better Diagnosis: An Overview

Maruturi Haribabu[1], Velmathi Guruviah[1,*] and PratheepanYogarajah[3]

[1]*School of Electronics Engineering, Vellore Institute of Technology, Chennai, India;* [2]*School of Computing, Engineering and Intelligent Systems, Ulster University, United Kingdom (UK)*

ARTICLE HISTORY

Received: January 07, 2022
Revised: March 28, 2022
Accepted: April 07, 2022

DOI:
10.2174/1573405618666220606161137

Abstract: Medical imaging plays a vital role in medical diagnosis and clinical treatment. The biggest challenge in the medical field is the correct identification of disease and better treatment. Multi-modal Medical Image Fusion (MMIF) is the process of merging multiple medical images from different modalities into a single fused image. The main objective of the medical image fusion is to obtain a large amount of appropriate information (*i.e*., features) to improve the quality and make it more informative for increasing clinical therapy for better diagnosis and clear assessment of medical-related problems. The MMIF is generally considered with MRI (Magnetic Resonance Imaging), CT (Computed Tomography), PET (Positron Emission Tomography), SPECT (Single Photon Emission Computed Tomography), MRA (Magnetic Resonance Angiography), T1-weighted MR, T2-weighted MR, X-ray, and ultrasound imaging (Vibro-Acoustography). This review article presents a comprehensive survey of existing medical image fusion methods and has been characterized into six parts: (1) Multi-modality medical images, (2) Literature review process, (3) Image fusion rules, (4) Quality evaluation metrics for assessment of fused image, (5) Experimental results on registered datasets and (6) Conclusion. In addition, this review article provides scientific challenges faced in MMIF and future directions for better diagnosis. It is expected that this review will be useful in establishing a concrete foundation for developing more valuable fusion methods for medical diagnosis.

Keywords: Multi-modality, medical images, medical image fusion, diagnosis, image fusion rules, quality assessment metrics.

1. INTRODUCTION

In past decades, medical image fusion provides an extraordinary improvement in medical imaging aspects. MMIF is the combination of different modalities of medical images into a single image with more quality and visualization [1]. The multi-modal medical images are MRI, T1-weighted MR, T2-weighted MR, CT, PET, SPECT, MRA, X-ray, and ultrasound imaging, which can be obtained from various sensors with different geometry. The ultimate goal of MMIF is to extract more complementary and relevant information from source images for better diagnosis. In medical image fusion, image registration plays a significant role in better image analysis. Image registration is the first step in image fusion to register the source images. It is defined as the process of alignment of source images with respect to the reference image. This process requires two images as input: the original image is called a reference image, and the image that will be aligned with the reference image is called a sensed image. The purpose of this type of alignment is to match related images based on particular features to help in the fusion process. In general, the registration framework is viewed as an optimization issue with the goal of increasing similarity or lowering cost. In medical imaging, the registration process enables to merge information from various modalities such as MRI, T1-T2 weighted MR, CT, PET, SPECT, MRA, X-ray, and ultrasound to get complete information about the patient, and aid in identifying the disease, to facilitate treatment verification.

Therefore, the image registration process is required in the medical field because these registered images are well-suited for medical image fusion to achieve a better diagnosis, and complete the fusion process successfully [2, 3].

An MRI image is created by radio waves, which provides the delicate tissue data related to human organs with high spatial resolution and plays an important role in the investigation of non-invasive diagnosis of the human body. An MRI image is used to detect and diagnose various medical-related issues such as traumatic brain injury, brain tumours, multiple sclerosis, blood vessels, bones, pelvis, joints, developmental anomalies, brain hemorrhage, dementia, infection, stroke, and the causes of headache, spinal tumours, spinal cord compression, herniated discs, and fractures. In addition, the application area of MRI image is color extraction, shape and structure of specimen, lung cancer disease treatment, surgical planning and training, liver disease, *etc*. The main advantage of the MRI image is its clarity in providing information about the fetus of the pregnant woman without exposing them to any kind of radiation. But it can not provide tumour-related information of the fetus if

*Address correspondence to this author at the School of Electronics Engineering, Vellore Institute of Technology, Chennai, India;
E-mail: velmathi.g@vit.ac.in

1573-4056/XX $65.00+.00

any. MR-T1 image provides soft tissue information but does not detect the abnormalities. However MR-T2 image can provide information of the thickness of the tumour region.

A CT image provides hard tissue information and it is an important imaging technique in the medical diagnosis and evaluation field. CT scans are preferred by doctors for diagnoses of various diseases, namely, colonography, vascular condition, muscle diagnosis, bone fractions and tumours, and blood clot. It also helps in surgery, radiation therapy, and the detection of the location and size of the tumour, as well as the internal bleeding and injuries. The other application areas of CT images are head cancer detection, neck and vulvar cancer diagnosis, bone cancer identification and treatment, liver tumour diagnosis, esophageal cancer diagnosis, lung cancer diagnosis, and surgical treatments. The short scanning time with high resolution and greater depth of penetration are the advantages of CT imaging, but it faces difficulty in tissue characterization.

PET image is a molecular imaging technique with high sensitivity, which provides the functionality of tissues and organs with low resolution. The PET scan is used to diagnose dementias (Alzheimer's disease), and other neurological conditions such as Parkinson's disease, Huntington's disease, Epilepsy, Cerebrovascular accident (stroke), hematoma (blood clot), and bleeding. The application areas of PET image are cancer treatment, tumour detection and treatment, and lung and breast cancer diagnosis. The advantage of PET image is its greater depth of penetration, but it is a highly expensive technique.

SPECT image is a nuclear imaging technique and mainly used for studying the flow of blood to organs and tissues. The SPECT images are commonly used to diagnose brain disorders, heart problems, and bone disorders. The other applications include prostate cancer treatments, pelvis irradiation detection and treatment, colorectal and vulvar cancer treatment, assessment of breast cancer, tumour detection, liver cancer diagnoses, neck and head cancer diagnosis, brain diagnosis, and treatment, *etc*. The advantage of SPECT image is its greater depth of penetration, but the major challenging issue is its improving sensitivity without loss of image quality. MRA image consists of a powerful magnetic field, used to evaluate blood vessels and identify abnormalities in the brain, but does not provide soft tissue information [4-13].

William Rontgen discovered X-rays on 8th November 1895 and used them to create the body's "shadow grams". Radiography is the use of X-rays to image the internal organs. An X-ray image can provide bone and fractural information of the human body. Mammography is one of the X-ray-based methodologies, which is used to assess breast cancer but does not provide the thickness of the disease object. The ultrasound image is a sonar-based imaging technique, used in different diagnostic application areas such as breast cancer detection, prostate cancer treatment, liver tumour, and esophageal cancer diagnosis, *etc*. The greater spatial resolution and low cost are the advantages of ultrasound imaging, but the limitations are operator dependent and challenging images of lungs and bones.

Vibro-Acoustography is another type of ultrasound imaging methodology, which is useful for detecting the thickness of the disease object and abnormalities in the breast but

Table 1. Various application domains in the medical field [9, 13, 14].

Organs	The Functionality of Medical Images	Fusion Combinations
Brain	MRI: It provides soft tissue information. CT: It provides bone information, *i.e*., hard tissue. PET: It is used to measure the activity of the brain by showing the blood flow in functional brain tissues. SPECT: It is utilized to quantify the progression of blood in the human brain.	CT-MRI, MRI-PET, PET-CT, MRI-SPECT, CT-SPECT, MR-T1-T2
Breast	MRI: Identification and detection of breast cancer. PET& SPECT: It is used to accurately identify breast tumours and detect early breast cancer. Ultrasound: Detects the abnormalities in the breast. X-ray: It is used for the assessment of breast cancer.	MRI- PET, X-ray -VA.
Prostate	MRI: Location and visualization of the prostate area. CT: Pretreatment evaluation and identification of cancer nodes. Ultrasound: Identifies the location of cancers in the gland. PET: It is used to detect ambiguous metastases in prostate patients' cancer by measuring the metabolic rate of tissue	CT-MRI, CT-PET.
Lungs	MRI: It is used for a better diagnosis of pulmonary hypertension. CT: It is used for tumour detection. X-ray: It is used for better diagnosis. PET: It is used for the diagnosis of non-little cell bronchial carcinoma.	CT-PET, MRI-PET.
Liver	MRI: It is used to detect the lesion. PET: It is used for the early detection of tumuor abnormalities and localization. CT: It is used to acquire various phases of tissue for lesion identification. Ultrasound: Offers a fast-noninvasive technique for observing suspected liver metastases	CT-PET

does not provide fraction information. Above all, the cost involved is one of the important criteria in the medical field. MRI and CT images are of intermediate cost; PET and SPECT are of high cost, while X-ray and ultrasound images are of comparatively low cost. The MR-T1 and MR-T2 are of intermediate cost [13, 14]. Regarding this information, each medical image has its own merits and limitations, as shown in Table **1**.

The combination of various multimodal medical images is a required criterion in the medical field, as shown in Fig. (**1**) because each modality provides limited information, which is not suitable for better diagnosis. In Fig. (**1**), the source images are obtained from the whole brain atlas website, and the fused image is suitable for better diagnosis, such as clear identification of tumour regions and abnormalities of the brain.

Three levels of operations are performed in image fusion techniques [15, 16]. In the pixel level, the images of individual pixels are directly combined. In the feature level, the extract of an image is featured through the region-based scheme, and in the decision level, the operations between the regions of images with consideration of detection and classification of the object are considered. The representations of three levels are observed in Fig. (**2**).

In this review article, various examples of medical image modalities have been presented and discussed, as shown in Fig. (**1**). The first row of medical images shows MRI and CT, which are taken from the image fusion toolbox for Matlab 5.x [17]. The second row of medical images shows MRI and PET, which represent the disease, namely, neoplastic disease (brain tumour). The third row of medical images shows MRI & SPECT, which represent Degenerative Disease (Alzheimer's disease) [18]. The fourth row of images shows CT and PET, which are used for lung cancer diagnosis [19]. The fifth row of medical images shows T1-MR and MRA, which are used for the identification of lesion locations with structure data [20]. The sixth row of medical images shows vibro-acoustography (VA) and X-ray mammography images that help in breast cancer diagnosis [21]. The seventh row of medical images shows T1-T2 weighted MR images, which are used for sarcoma diagnosis [18].

2. LITERATURE REVIEW

This section provides a detailed review of MMIF research and the author's contributions. Medical image fusion is classified into various fusion methods that are shown in Table **2**. In this literature study, methodologies such as IHS (Intensity-Hue-Saturation) fusion, pyramid, transform related methods, salient feature detection, sparse representation methods, deep learning, fuzzy set, hybrid and optimization based fusion methods have been studied and discussed in detail for better diagnosis of medical related problems.

2.1. Intensity-Hue-Saturation

The IHS-based fusion method [22-24] provides a better-quality image with beautiful color visualization and spatial resolution. The procedure for HIS image fusion has two

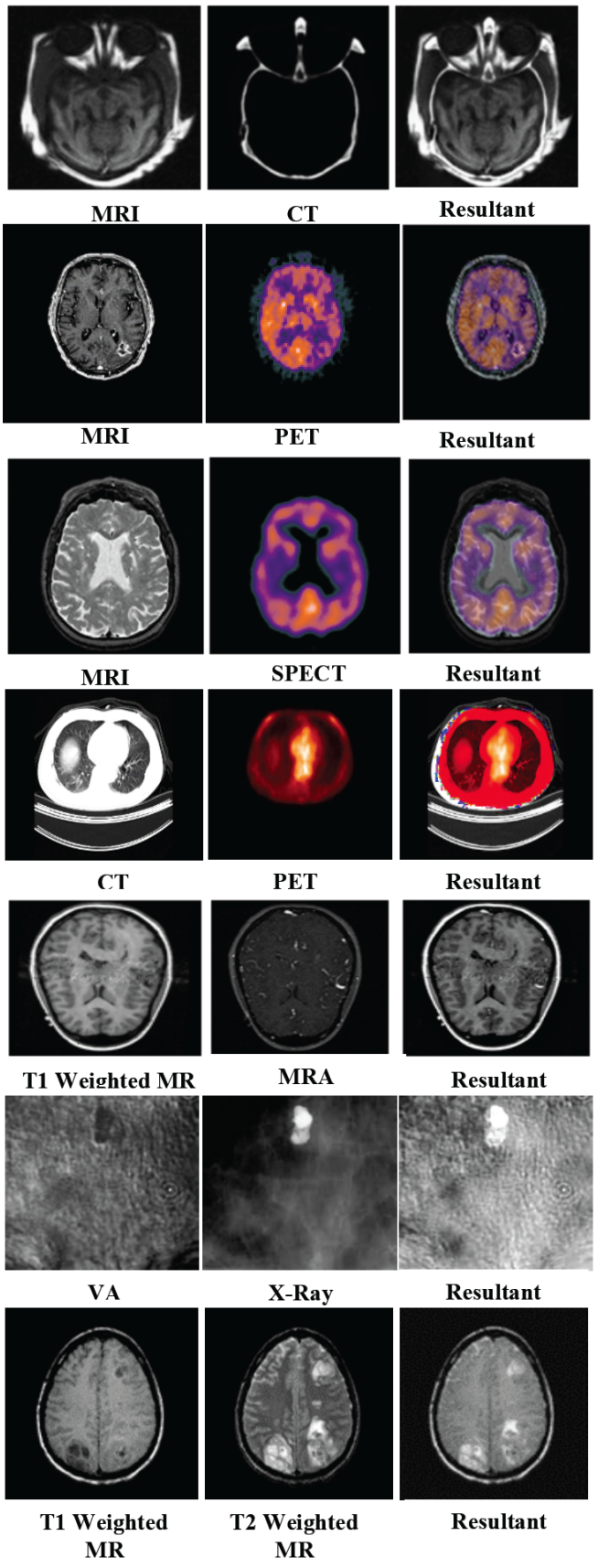

Fig. (1). Examples of MMIF with fused images [17-21]. (*A higher resolution / colour version of this figure is available in the electronic copy of the article*).

Table 2. Classifications of MMIF methods.

Methods	Techniques	References
Image Decomposition and Reconstruction	➢ Intensity-hue-saturation (IHS)	[22-24]
	➢ Pyramid based fusion methods	[25-26]
	➢ Transform domain-based methods:	
	1. Discrete wavelet transforms (DWT)	[27-30]
	2. Redundant wavelet transforms (RWT)	[31-32]
	3. Multi wavelet Transform (MWT)	[33]
	4. Lifting wavelet transform (LWT)	[34]
	5. Dual-tree complex wavelet transform (DT-CWT)	[35]
	6. Curvelet Transform (CVT)	[36]
	7. Contourlet Transform (CONT)	[37-38]
	8. Non-Subsampled Contourlet Transform (NSCT)	[39-43]
	9. Shearlet Transform (ST)	[44-46]
	10. Non-Subsampled Shearlet Transform (NSST)	[47-49]
	➢ Sparse representation	[50]
	➢ Salient feature-based methods	[51-56]
Deep learning	➢ Convolution neural network (CNN)	[57-66]
Fuzzy Set	➢ Fuzzy sets, Intuitionistic fuzzy sets	[67-78]
Hybrid and optimization	➢ Combination of multiple techniques	[79-103]
Other fusion methods	➢ ICA, Support vector machine (SVM), *etc*.	[104-110]

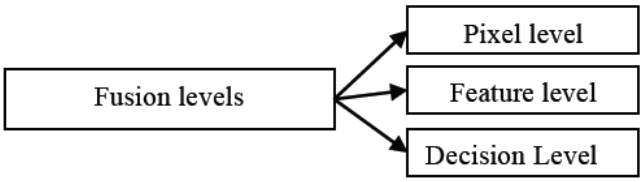

Fig. (2). A Dynamic classification of image fusion levels.

steps: i) Converting the colored RGB image into the IHS model by using Eq. (**1**, **2**) to get a new intensity image. ii) Obtaining the fused image by IHS-RGB transformation by using Eq. (**3**), *i.e*., reconstruction process. The diagrammatic representation of IHS-based medical image fusion is shown in Fig. (**3**).

The color space method is performed in two steps:

(1) The mathematical modelling of RGB- IHS:

$$I_1 = \frac{R_1 + G_1 + B_1}{3} \quad (\mathbf{1})$$

$$\begin{cases} H_1 = \dfrac{G_1 - B_1}{3I_1 - 3B_1} \;,\; S_1 = \dfrac{I_1 - B_1}{I_1} \;,\; if \quad B_1 < R_1, G_1 \\ H_1 = \dfrac{B_1 - R_1}{3I_1 - 3R_1} \;,\; S_1 = \dfrac{I_1 - R_1}{I_1} \;,\; if \quad R_1 < B_1, G_1 \\ H_1 = \dfrac{R_1 - G_1}{3I_1 - 3G_1} \;,\; S_1 = \dfrac{I_1 - G_1}{I_1} \;,\; if \quad G_1 < R_1, B_1 \end{cases} \quad (\mathbf{2})$$

(2) IHS–RGB transformation to get the final image:

$$\begin{cases} R_1 = I_1\left(1 + 2S_1 - 3S_1 \times H\right) \;,\; G_1 = I_1\left(1 - S_1 + 3S_1 \times H\right) \;,\; B_1 = I_1\left(1 - S_1\right) \;,\; if \quad B_1 < R_1, G_1 \\ R_1 = I_1\left(1 - S_1\right) \;,\; G_1 = I_1\left(1 + 5S_1 - 3S_1 \times H\right) \;,\; B_1 = I_1\left(1 - 4S_1 + 3S_1 \times H\right) \;,\; if \quad R_1 < B_1, G_1 \\ R_1 = I_1\left(1 - 7S_1 + 3S_1 \times H\right) \;,\; G_1 = I_1\left(1 - S_1\right) \;,\; B_1 = I_1\left(1 + 8S_1 - 3S_1 \times H\right) \;,\; if \quad G_1 < R_1, B_1 \end{cases}$$

(**3**)

Here, R_1, G_1, and B_1 are red, green, and blue components, and H_1, S_1, and I_1 are the Hue, Saturation, and Intensity components, respectively. In color-based image fusion, researchers propose various combinations with IHS to get a valid visual quality image for a better diagnosis of tumours and their possible treatment.

2.2. Pyramid Based Fusion Methods

Pyramid based methods [25, 26] have been used in medical image fusion to represent better spectral information. The quality of a fused image depends on its decomposition levels. As the decomposition levels increase, the image quality also increases and vice-versa. Jiao Du *et al*. [25] proposed a Laplacian pyramid with multiple features based on medical image fusion. Initially, the input images are decomposed into multi-scale representations by using the Laplacian pyramid that is used to extract outline feature maps. Those features are to be fused with the weighted fusion rule. Finally, the fused image is obtained by inverse Laplacian and provides an enhanced outline, but it fails in terms of visualization. In morphological pyramid-based medical image fusion [26], the fused image is generated with more

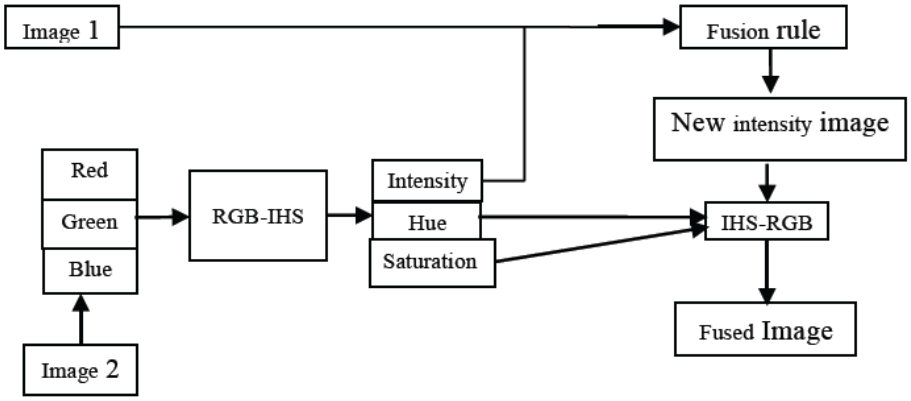

Fig. (3). Diagrammatic representation of IHS-based medical image fusion [22-24].

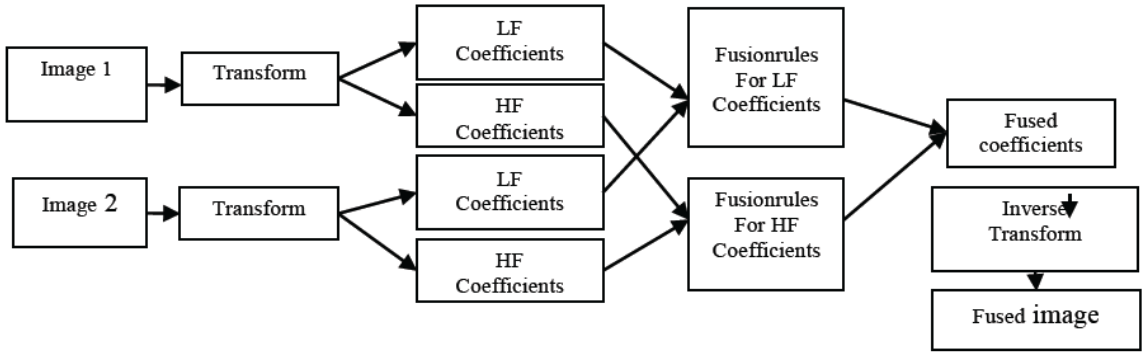

Fig. (4). A framework of transform-based MMIF [27].

spectral information. But pyramid-based methods are not much preferred due to blocking effects, artifacts, and edge uncertainties, that occur by sampling operation. Transform-based fusion methods provide better solutions for this problem.

2.3. Transform-based Fusion Methods

The transform-based fusion methods enhance the accuracy of a fused image with multi-resolution and lead to a better clinical diagnosis and treatment. Initially, the input images are decomposed into low band and high band frequency coefficients. Then, different fusion rules are applied to those bands to select quality fused coefficients. Lastly, the accurate fused image is generated by the inverse transformation. The diagrammatic representation of a transform-based medical image fusion is shown in Fig. (**4**). The transform-based fusion methods provide better fusion performance than the spatial domain methods.

The familiar transform-based fusion method is a Wavelet Transform (WT). Yong Yang *et al*. [27] proposed an efficient DWT based medical image fusion, which represents a pixel-based image fusion where wavelet coefficients are fused with visibility fusion rules to provide good localization and improve the resolution by windowing-based consistency verification. Rajiv Singh *et al*. [28] proposed wavelet transforms-based MIF. This technique is superior to pyramid-based methods, PCA, and the fused image has more complementary information. A. Anoop Suraj *et al*. [29] suggested a DWT based image fusion and denoising in FPGA. In this method, the input images are properly registered with affine transform, and then DWT. The selection of frequency bands is made using the least support vector machine, which removes the blurriness and artifacts. S. V. Jagadeesh Chandra *et al*. [30] proposed a DWT-based medical image fusion in which the author improves the fused image quality with more resolution and fewer artifacts.

The WT based image fusion preserves the information with effective localization in both spatial and spectral domains. However, this method fails to satisfy the shift-invariant due to the down sampling operation. This problem is solved by the redundant discrete wavelet transform (RDWT) [31, 32]. The authors P. S. Gomathi *et al*. [31] proposed medical image fusion based on RDWT with morphological operators. The fusion method provides a better analysis of medical modalities, which includes better component information, and is suitable for computer-aided- applications. H.N. Yadav [32] proposed an RDWT-based medical image fusion for computer-aided diagnosis. Initially, the input images are properly registered by mutual information, and then coefficients are fused by the entropy-based fusion rule, which leads to improve the quality of the fused image. This algorithm is used for the robustness of the fusion process to avoid merging artifacts of wavelet coefficients and is better than the traditional DWT methods, but it does not provide the required edge information. Multi Wavelet Transform (MWT) [33] is used to solve the shortcomings of the scalar wavelet. It has more texture and provides detailed information of a fused image, but it does not

provide the smoothness of edges. Lifting Wavelet Transform (LWT) [34] construction is divided into Spilt, Prediction, and Update phases, and it is famous for reducing the complexity in DWT, but with vagueness in edges. Heba.M. EI Hoseny *et al*. [35] proposed a DT-CWT based medical image fusion with an optimization algorithm and histogram matching. This fusion method provides a better visual quality image, and and is better than other conventional DWT based methods in terms of both qualitative and quantitative features. But the Wavelet-based fusion methods do not provide sufficient information such as the smoothness of edges, contours, and directionality of the images.

The Curvelet Transform (CVT) is an extended version of the conventional wavelet transform. Shirin Hajeb Mohammad Alipour *et al*. [36] proposed a CVT-based MRI-PET medical image fusion, where the input images are decomposed into frequency coefficients using discrete curvelet transform, and then regional information entropy is used to calculate the fused coefficients with the help of a maximum rule. The fused image is obtained by an inverse curvelet transform and this algorithm gives a fused image with sufficient curves and edges. However, this method is not sufficient for medical images due to its lack of directionality. This problem was addressed by Contourlet Transform (CONT) [37, 38], for better representation of an image with good contours and also to acquire a fine geometrical structure of an image. CONT has two functions such as the Laplacian Pyramid (LP) and Directional Filter Banks (DFB). LP identifies discontinuity points in the image and is linked by DFB for better directionality. L. Yang *et al*. [37] proposed a geometric analysis of CONT-based MMIF. The low fused coefficients are obtained by energy-based fusion rule and high fused coefficients are obtained by region weighted selection rule for extracting the features, such as edges, contours, sharp boundaries, and directionality. Hui Huang *et al*. [38] suggested a nonlinear approximation of contourlet transform-based image fusion for highlighting the edges and improving the efficiency. The source images are decomposed into coefficients, and then fused by a feature mapping algorithm. The feature mapping algorithm is used to remove the blocking effects, and provides the edges data. The obtained fused image has higher directionality with good contours. The CONT does not satisfy the shift-invariant, and this problem was well handled by a non-subsampled contourlet transform [39-43].

Gaurav Bhatnagar *et al*. [39] proposed a multi-modal medical image fusion using directive contrasts in the NSCT domain. This algorithm gives visual content with high contrast fused images without color distortions and is also useful to physicians for disease diagnosis in a better way. Guocheng Yang *et al*. [40] proposed statistical measurements of NSCT based MMIF. The low and high band coefficients of NSCT are fused using Shanon entropy and a weighted map, is used for extracting the salient features with structural information. These salient features are more needed for medical images for better diagnosis. Gaurav Bhatnagar *et al*. [41] suggested a multi-modal medical image fusion using a new contrasting NSCT. In this algorithm, the low and high fused coefficients are obtained by weighted matrix and sum modified Laplacian for the extraction of saliency information and edges. This algorithm leads to more resolution with high structural information in the fused image and is superior to DWT, CONT, and NSCT. Periyavattam Shanmugam Gomathi [42] proposed NSCT-based MMIF. The input images are decomposed into a low band and high band frequency coefficients for multi-resolution purposes. Mean and variance are the fusion rules used to select the best directionality and edge information from coefficients. Then the fused image is generated by inverse NSCT. This algorithm gives a 50% improvement compared to the other existing transformation methods. Zhiqin Zhu *et al*. [43] proposed NSCT with phase congruency and local energy-based MMIF. This method gives enhanced fused image with better structure and features. The NSCT-based fusion methods provide a fused image with more directionality, but it has more complexity and less sensitivity. To achieve better fusion results, which include more directionality with less complexity and high sensitivity, ST and NSST techniques are preferable.

The ST [44-46] and the NSST [47-49] are the most effective methods for fusing multi-modal medical images with detailed sparse directional representations, which include an infinite number of directions and complexity reduction than NSCT. The comparison of transform domain-based techniques is shown in Table **3**. In medical image fusion, the fusion performance can be improved by a hybrid combination of transform domain-based methods, as discussed in section 2.8.

2.4. Sparse Representation Based Fusion Methods

Sparse Representation (SR) is an efficient tool for better analysis of the human visual system and is used in various application areas such as face recognition, object tracking, image fusion, machine learning, *etc*. [50].

The procedure for Joint SR-based multi-modal medical fusion is shown in Fig. (**5**):

1. Initially, the source images are converted into vectors through a sliding window.
2. The vector representation of two source images sparsely by over-completes dictionary D.
3. The fused sparse coefficients are obtained by fusion rule and then converted into fused vectors using over-complete dictionary D.
4. Finally, the fused image is obtained with high resolution by reverse operation of step 1.

The dictionary can be created in two types: (1) fixed methodology, (2) learning methodology. The learning method was more efficient and flexible than the fixed method. The efficient construction of a learning-based dictionary is the K-SVD algorithm. The sparse representation based fusion method [50] does not provide the required edges and contrast of the fused image. In medical image fusion, many authors proposed various combinations with SR to obtain fused images with more visual and detailed information, and low distortions.

2.5. Saliency Feature-Based Fusion Methods

Saliency feature-based methods are quite different than the other fusion methods. The merits of this method are: (1)

Table 3. General Comparison of transform-based fusion methods.

Methods	LF Bands	HF Bands	Merits	Demerits
Wavelet Transform	One	Three	Good localization in both time and frequency	It does not provide edges, Contours, and directionality data.
Contourlet Transform	One	Finite	Produced sufficient edges and directionality.	It does not satisfy the shift-invariant due to down sampling.
Shearlet Transform	One	Infinite	It provides detailed sparse directional representation.	It leads to misregistration due to the lack of shift-invariant. NSST is a better way to handle this.

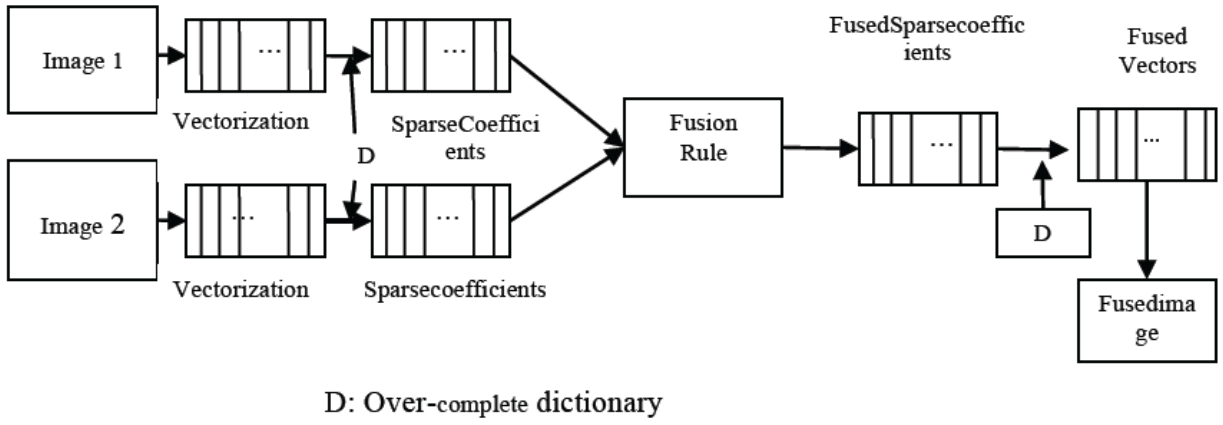

Fig. (5). Flow chart for joint sparse representation based medical image fusion [50].

saliency features extraction, (2) shift-invariance, and (3) low complexity. The diagrammatic representation of the fusion process is shown in Fig. (**6**).

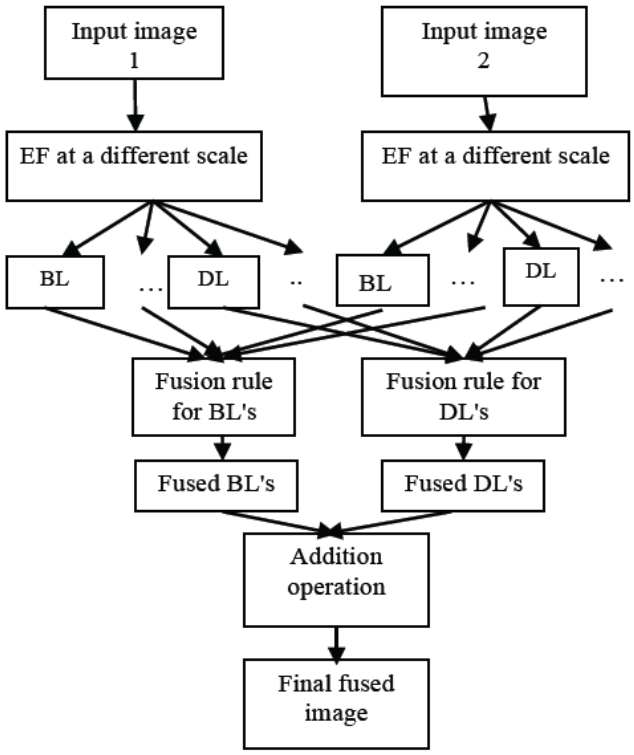

Fig. (6). Flow chart for an edge-preserving filter with saliency feature-based fusion method.

The edge-preserving filters play a wider role in medical image fusion for edge features such as Cross bilateral filter (CBF) [51], guided filter (GF) [52, 53], weighted least squares filter (WLSF) [54], Rolling guided filter (RGF) [55], and Fast guided filter [56]. These filtering techniques are used to produce detailed edges and better visual quality of the fused image. Recently, the researchers used these saliency-based image fusion methods as a preprocessing step at the initial stage of medical image fusion for noise reduction and enhanced edges.

The whole procedure showing the edge-preserving filter-based image fusion is summarized as follows:

Initially, the input images (I_1, I_2) are represented in various scales by edge-preserving filters (*EF*). The base layers (BL_1, BL_2) and detailed layers (DL_1, DL_2) of two images at different scales (i^{th} *level*) are computed by Eqs. (**4**, **5**).

$$BL_i^1 = I_1 * EF_i$$
$$BL_i^2 = I_2 * EF_i \quad (4)$$

$$DL_i^1 = I_1 - BL_i^1$$
$$DL_i^2 = I_2 - BL_i^2 \quad (5)$$

The effective fusion rule is used to fuse both base and detailed layers by Eq. (**6**).

$$BL_F = fu_B(BL_i^1, BL_i^2)$$
$$DL_F = fu_D(DL_i^1, DL_i^2) \quad \textbf{(6)}$$

Where BL_F and DL_F are the fused base layer and detailed layer, and fu_B, and fu_D are fusion rules regarding the base layer and detailed layer, respectively. Finally, the fused image is obtained by Eq. (**7**).

$$I_{fu} = BL_F + DL_F \quad \textbf{(7)}$$

2.6. Deep Learning Based Fusion Methods

In recent years, deep learning has emerged as a new era in the medical field for disease diagnosis. Aprominent and typical deep learning model is the Convolutional neural network, because it is a class of deep neural networks, and is most widely used to analyze visual imagery. The convolutional neural network is multistage feed-forward ANN, and the convolution operation is multidimensional. It derives its name from the form that it consists of multiple hidden layers, such as convolutional layers, pooling layers, completely linked (fully connected) layers, and normalized layers. The first parameter of CNN is input, and the second parameter is kernel, and the last parameter is output, which lead to generate a feature map. The spatial and transform domain-based medical image fusion methods have flaws in the extraction of detailed features and fusion rules, which requires artificial design. The CNN based image fusion provides a fused image with more detailed features and better visual quality. The deep learning is used in various medical application areas such as classification [57], medical diagnosis [58], segmentation [59-61], image fusion [62-65], and image registration [66].

Various authors suggested image fusion algorithms related to CNN with better fusion rules, such as Yu Liu et_.al. [62] proposed Deep CNN based image fusion. This architecture extracts the high-frequency details from source images using filters and then performs CNN to generate a focus map. This focus map is used to provide optimized details with consistency verification for better visualization and quality. Haithem Hermessi *et al*. [63] suggested a new CNN and Shearlet domain based medical image fusion. This proposed method extracts the features with better visualization of a fused image *via* a similarity learning scheme and fully connected Siamese architecture in the NSST domain. Weighted NCC based feature maps are generated by CNN, which are used in the fusion of high-frequency coefficients and the low-frequency fused coefficients are obtained by the energy-based fusion rule. The fused image is superior to traditional NSST methods in terms of visualization and directionality. Ruichao Hou *et al*. [64] proposed an MRI-CT medical image fusion using CNN and DCSCM (Dual-channel spiking cortical model). Their methodology is related to feature-based image fusion. Initially, two medical images are decomposed into coefficients by NSST. The low and high frequency fused coefficients are obtained by the CNN based feature map with adaptive selection rule and DCSCM. The DCSCM is used to extract textures, and detailed information from the dark regions. After that, a better and more detailed fused image is produced by inverse NSST.

Meng Wang *et al*. [65] suggested image fusion based on supervised deep learning CNN with weighted gradient flow. The salient features were extracted, and integrated by back propagation gradients, and then fusion rule was performed with weighted gradient flow, which improved the detailed structural information. This proposed deep network was tuned according to the pre-trained network such as VGG 16, VGG 19, and ResNet 50. This fusion method provides superior results than the other existing techniques such as NSCT, SR, GF, *etc*. The deep learning based fusion method provides a fused image with more features, and efficient edge information, but it faces various difficulties such as lack of training datasets, complexity in network framework, high cost, and long training time.

2.7. Fuzzy Set Based Fusion Method

Generally, medical images are poorly illuminated and even some details will not be visible *i.e*., vagueness in nature. In medical image fusion, enhancement has a prominent role in the clarity of disease identification without ambiguity. Several enhancement techniques such as histogram [67], gray-level transform [68] based methods, *etc*., have been proposed, but they are not sufficient for medical image fusion, because of their uncertainties. This problem was solved by a mathematical tool called a fuzzy set [69]. Fuzzy sets are used to remove vagueness but not to handle more uncertainties since they contain only membership functions [0, 1]. The generalized version of a fuzzy set is the Intuitionistic Fuzzy Set (IFS) [70]. IFS considers more uncertainties.

Ruche Sanjay *et al*. [71] proposed DWT and fuzzy logic based medical image fusion. In this algorithm, low fused coefficients are generated by fuzzy logic and high fused coefficients are generated by the average rule. This algorithm is used to remove the vagueness present in the medical image. The final fused image is obtained by inverse DWT and it is superior to other pyramidal based methods. Balasubramanian *et al*. [72] suggested IFS based image fusion. This method provides a fused image without uncertainties and it is superior to other transformation techniques. The author proposed [73-76] Intuitionistic fuzzy set based multi-modal medical image fusion techniques. These algorithms provide bright and contrast-enhanced fused images with detailed structures. These methods are superior to Non-fuzzy techniques both qualitatively and quantitatively. T. Tirupal *et al*. [77, 78] proposed Sugeno's and Yager's IFS based medical image fusion. These algorithms give enhanced fused images with a clear structure of the tumour present.

2.8. Hybrid and Optimization Algorithms Based Medical Image Fusion

Recently, many researchers have proposed and published hybrid and optimization algorithms based fusion techniques [75, 79-103], which lead to improved fusion performance in terms of visual quality. It also provides quantitative analysis for better diagnosis and assesses medical-related problems, such as Rajkumar Soundrapandiyan *et al*. [75] proposed DWT and Intuitionistic fuzzy set (IFS) based medical image fusion. Initially, the input images are fused by using DWT with maximum and entropy-based fusion rules. The initial fused images have a lot of uncertainties,

and those are overcome by the intuitionistic fuzzy set. The final fused image has high contrast without uncertainties. Jyothi Agarwal *et al*. [79] proposed DWT and curvelet transform-based image fusion. This hybrid technique provides a fused image with good localization and better edges, and is superior to conventional DWT and CVT based techniques, but does not provide directionality information. Yin Dai *et al*. [80] proposed medical image fusion based on wavelet, pseudo-color, and α channel fusion methods, used to highlights the in-depth details and clear visible lesions of cerebral infractions in a fused image. Jing-Jing Jong *et al*.[81] proposed an SR based Medical image fusion. The input images are split into patches over a dictionary, and each patch can be represented sparsely by the least angle regression algorithm, which leads to better resolution. The sparse coefficients are fused using the maximum fusion rule, and the fused image is reconstructed from combining fused sparse coefficients with the corresponding dictionary. This fusion process has been proved better than the DWT, NSCT, and SR methods both visually and quantitatively. Nargis Aktar *et al*. [82] proposed hybrid medical image fusion, which includes DTCWT and PCA. The DTCWT is used to extract saliency features from input images and PCA is used to compute principal components, which are used in the processing of that features and that reduce the redundant information, which is generated by DTCWT decomposition. This method is superior to PCA, DWT, DTCWT, DWT+PCA methods. Ebenezer Daniel *et al*. [83] proposed an optimum spectrum mask and GWO (Gray wolf optimization algorithm) based on medical image fusion. The optimum spectrum mask is used to obtain better contrast, edge information, and minimize the redundancy of fused images.

Jingming Xia *et al*. [84] presented a hybrid medical image fusion, which includes SR, NSCT, and PCNN. Initially, the two input images are decomposed into low and high coefficients by NSCT. Then, the low-frequency coefficients are fused by sparse representation, and fused high-frequency coefficients are obtained by PCNN, which is helpful to extract meaningful features and detailed edge information. Finally, the fused image is obtained by inverse NSCT with detailed information regarding the structure and edges, and is superior to NSCT, SR, NSCT-SR, and NSCT-PCNN techniques, but the major drawback is parameters' setting in the conventional PCNN. Ebenezer Daniel [85] suggested an optimum wavelet-homomorphic and genetic gray wolf optimization algorithm (OWHF+HG-GWO) based on medical image fusion. Firstly, registered input images are enhanced by homomorphic filtering and then decomposed using DWT to get approximation and detail coefficients. Secondly, the approximation and optimized detail coefficients of the first image, and detail and optimized approximation coefficients of the second image are added and vice versa. The optimized scale values are selected by the HG-GWO. Lastly, according to the reconstruction process, the fused image is obtained. This method is suitable for all medical datasets.

Ling Tan *et al*. [86] proposed fast finite Shearlet transform and SR-based medical image fusion. The author's contributed work represents a quality fused image with directionality, and better visualization, and is 35% superior to the state-of-the-art fusion methods such as NSCT, NSST, *etc*. Mehdi Hassan *et al*. [87] suggested neuro-wavelet based MIF. The low and high frequency coefficients are fused by using the neural network with extracted features. The fused image is obtained by inverse DWT, and gives better results both visually and quantitatively. Sharma Dileep Kumar Ramlal *et al*. [88] proposed hybrid based medical image fusion. This method resolves the limitations of individual NSCT and SWT. The fused image has more texture, point discontinuities, and good edge information. B. Rajalingam *et al*. [89] presented a DT-CWT with NSST based MIF. However, the combination of two techniques produced a quality fused image with more detailed information. Chenxi Huang *et al*. [90] contributed work related to NPCNN and optimized by the shuffled frog leaping algorithm (SFLA). The low and high frequency bands of NSCT are fused by SFLA-PCNN fusion rule. In the PCNN model, it is difficult to handle the parameters setting. To overcome that problem, SFLA is used for optimizing the PCNN parameters. This proposed method gives a quality fused image; robustness and the tumour region are visible clearly.

Jun Li *et al*. [91] suggested guided filter and ORDL (online robust dictionary learning) based image fusion. The guided filter is an edge preserving filter, used to amplify the edge information, and a jointly clustered patch ORDL algorithm is used to reduce the amount of training data and improve the performance of the fusion process. The author's proposed method is better than the MST (Multiscale Transform) and MST-SR based methods. Heba M. EI-Hoseny *et al*. [92] contributed work based on medical image fusion using NSST, modified central force optimization (MCFO), and contrast enhancement. This method has four stages of operation. Firstly, perform histogram matching of both registered input images, and decomposed by NSST. Secondly, MCFO generates optimized gain parameters for better selection of features from coefficients and then fused. Thirdly, the fused image is obtained by the inverse NSST. Lastly, the contrast enhancement technique is used to enhance the fused image quality. Q. Hu *et al*. [93] proposed a dictionary learning and Gabor filter based MMIF. The frequency bands are fused by Gabor energy weights, and sparse representations, which are updated by dictionary-based algorithm (OMP) with manifold-based conjugate gradient method. The advantage of Gabor filter is to improve the image texture with frequency and direction representation, and the dictionary leads to non-unique solutions of the sparse matrix. This fusion process gives good fusion results over the NSCT-RPCNN, NSCT-PAPCNN, and NSST-SR based methods. Velmurugan Subbiah Parvathy *et al*. [94] proposed Optimization algorithm based medical image fusion, which includes DWT and Binary crow search optimization (BCSO) algorithm. The initial stage of fusion process is noise removal, which can be done by the median filter. After that, the DWT coefficients are fused by using optimized parameters, which are generated by the BCSO algorithm, and are used for the better selection of parameters. This methodology is superior to another optimization algorithm, such as genetic algorithm (GA).

Lina Xu *et al*. [95] proposed optimized DWT- homomorphic filter based medical image fusion. The enhanced coefficients are optimized by a shark smell optimization, which is used to select optimized parameters. The fused image has fine details and is superior to DWT, PCNN, DCT,

LP and IHS techniques. Yanyu Liu *et al*. [96] proposed Total-Variational-Decomposition (TVD) and Robust spiking cortical model (RSCM) based MMIF. The input images are decomposed into a base and detailed layer using TVD, and then fused by fusion rules, which include RSCM and CNN model. The fused image has good contrast, better detailed information, and high computation speed. Sarmad Maqsood *et al*. [97] proposed two-scale decomposition and sparse representation based MMIF. The input images subjected to pre-processing by contrast enhancement technique and then decomposed into a base and detailed layer. The fused image is obtained by a decision map, which is generated by a dictionary, and then reconstruction takes place. Zhaisheng Ding *et al*. [98] proposed Brain MIF based on dual channels CNNs in the NSST domain. The fusion strategy of this method is, that the initial weights are integrated into an input image by the CNN model, and then decomposed by NSST. The resultant fused image has better quality without distortion, and is superior to NSCT-PCNN, NSST-PAPCNN, SR-CVT, and NSST-SR methods.

Jingming Xia *et al*. [99] proposed NSST, PAPCNN, and CSR based image fusion, which is used to extract the structural and detailed features. This method gives better results in terms of qualitative and quantitative analysis, and is superior to traditional NSST-PCNN, CSR, SR-PCNN methods, *etc*. Padmavathi K *et al*. [100] suggested TV -L1 decomposition of MRI-PET MIF. The cartoon and texture components are fused with weights, which are generated by PSO. The fused image has more texture and visual details which are preserved with greater contrast, but the major drawback is high computation time. Yu Liu *et al*. [101] proposed convolutional sparsity with morphological component analysis (CS-MCA) based MIF. The input images are decomposed into cartoon and texture components and then fused by feature maps, which are generated by CS-MCA with the help of a dictionary. This method gives an improvement in diagnosis and better than the standard SR-based methods.

Kamal deep Kaur *et al*. [102] proposed Hilbert and gray wolf optimization algorithm-based MIF. The advantage of HT is extorting the information from input images and optimum spectrum scaling, which is used for the selection process, and used for removing the optimization problem in PSO.

Sneha Singh [103] suggested improvement of medical image fusion, which represents multi-layer decomposition such as base and detailed layers. The base layers are fused by a feature map, which is obtained by CNN with the regional energy fusion rule, and the detailed layers are combined using a cluster-based dictionary. The obtained fused image has high contrast of tumour regions with low computation time.

2.9. Other Fusion Methods

The dimensionality reduction based medical image fusion methods used for feature processing are PCA [104] and independent component analysis (ICA) [105]. Few authors proposed various approaches of medical image fusion for improvement of fusion performance for better medical diagnosis such as SVM (Support Vector machine) [106], AFSSD [107], FMI based medical image fusion [108], local extrema based medical image fusion [109], NPDM modal [110]. S.L. Jany Shabu [106] proposed a fusion method named SVM classifier for feature extraction and detection of tumour region. Arash Saboori *et al*. [107] proposed an adaptive filter based on medical image fusion with spectral and spatial discrepancy. The usage of an adaptive filter is to integrate both medical image information, and then fuse it by optimized parameters, which are generated by spectral and spatial discrepancy. This algorithm proves both subjectively and objectively better than DWT, IHS, and HPF methods. Li Yufeng *et al*. [108] proposed modulation-based image fusion. The input images are multiplied with a factor and then combined. The fusion performance is superior to DWT and LP. Zhiping Xu *et al*. [109] suggested medical image fusion based on multi-level local extrema for medical application, which includes local energy and contrast-based fusion rule. This technique shows better visualization, but edges are not enhanced properly. Zhe Liu *et al*. [110] suggested non-parametric density model for reducing the distortions and mismatch problems. The fused image of this method has good localization and abnormalities characterization. The comparison of existing techniques, which includes straight, hybrid, and optimization algorithm-based fusion methods is shown in Table **4**.

The aforementioned, each medical image fusion method has its own merits and demerits. Still, image fusion techniques require more efficient algorithms to exhibit fused image with more information, useful for better diagnosis, since fused image has many uncertainties and vagueness.

3. MEDICAL IMAGE FUSION RULES

In the medical image fusion process, the fusion rule plays an important role in highlighting the features of input images that are superimposed on the output image. The average and maximum rules are frequently used as pixel-based fusion rules. The image fusion rules mentioned in this literature are principal component analysis (PCA) [104], energy-based fusion rule [111, 112], human visualization based fusion rule [78], PA-PCNN based fusion rule [49], modified spatial frequency (MSF) fusion rule [113], IFS based cosine similarity [114], normalized weighted sum based fusion rule [115], consistency verification [78, 116], and phase congruency (PC) [117-119]. These rules are used to extract the image features to make decision for performing the fusion process.

3.1. PCA Based Image Fusion Rule

PCA based image fusion rule is related to highlight the invisible saliency features of an image. The best example is PCA, which is used as a dimensionality reduction tool to create weights by principal components. The procedure for weights calculation using PCA is as follows:

1) Let $R^1 and R^2$ are the two coefficients of input images

$$R^1 = \begin{bmatrix} y_1^1 \\ y_2^1 \\ . \\ . \\ y_n^1 \end{bmatrix}, \quad R^2 = \begin{bmatrix} y_1^2 \\ y_2^2 \\ . \\ . \\ y_n^2 \end{bmatrix} \tag{8}$$

Table 4. Comparison of existing medical image fusion method.

Fusion Methods	Modalities	Advantage	Disadvantage
IHS & PCA [22]	MRI-PET	Fused image has better color visualization and spatial features.	It causes spectral distortions at the boundaries and low contrast.
LP [25]	MRI -CT,	This method preserves better outlines in a fused image. Low complexity.	May introduce artifacts and blocking effects on fused image boundaries.
DWT [27]	MRI-PET,	It provides good localization in both time and frequency.	It has more complexity and does not satisfy the shift-invariant property.
RWT [31]	MRI-SPECT	Satisfies shift invariant property and good resolution.	Unable to reflect the edges information.
MWT [33]	MRI -CT	Increase the image analysis, texture information, and feature extraction.	Presence of noise at edges in a fused image.
LWT [34]	MRI -CT	Less complexity.	Fused image suffers with blocking effects at the outlines.
CVT [36]	MRI -CT	It covers sufficient curves and edges information.	Lack of directionality
CONT [37]	MRI -CT	More edges, directionality information is present in a fused image and superior than DWT & CVT.	May causes blocking effects and low contrast.
NSCT [43]	MRI, PET	Superior to traditional transform techniques in terms of directionality.	High complexity.
ST [44]	MRI -CT	This method provides a fused image with more directionality with less spectral distortions.	This method leads to misregistration due to lack of shift invariance.
NSST+PAPCNN [49]	MRI-CT,	Fusion process is Superior to NSCT with less complexity, and overcome the drawbacks in PCNN.	Low brightness and Contrast due to uncertainties, and high computational time.
JSP [50]	MRI-PET,	Fused image has less color distortions and blocking effects.	Does not provide a quality fused image, and the edges are not clear.
GF [52]	MRI-SPECT	This method gives noise free and preserves more detailed edge information in a fused image.	Visual representation is poor and provides CT image information.
CNN+ DCSCM [64]	MRI -CT	This method gives optimized parameters for selection of features from input images and produce fused image with clear tumor region.	High expensive and long training time.
YIFS [78]	MRI-CT, MRI-PET, MRI-SPECT	This method gives a better contrast fused image without distortions.	CT image information is not enhanced properly.
GWO+ OSM [83]	MRI-CT, MRI-PET, MRI-SPECT	Fast computation speed as well as dynamic selection of optimized scale values, and are used for better diagnosis.	Edges information is not up to level.
NSCT+PCNN+SR [84]	MRI -CT	This algorithm is suitable for gray and color images, and gives better results than conventional NSCT based techniques.	MRI information is not clear *i.e*., artifacts.
OWHF+HG-GWO [85]	MRI-CT, MRI-PET, MRI-SPEC	Fused image is obtained by optimized parameters, and suitable to various medical data sets.	High computation time and Low brightness.
NPCNN [90]	MRI-PET, MRI-SPECT	Overcome the drawbacks in PCNN, and provides optimization selection using fewer parameters.	Vagueness is present in a fused image.
GF+ORDL [91]	MRI -CT	This method provides better results in terms of edges than the SR and other MST techniques.	Soft tissue information is less in a fused image., and low brightness
BCSO [94]	MRI-CT, MRI-PET, MRI-SPECT	Complementary information is present in a fused image.	Less directionality information
TVD+SR [96]	MRI -CT	Provides better detailed information and high computation speed.	Some parts are not visible clearly in a fused image
DCNN+NSST [98]	MRI -CT	Enhance the contrast of diagnostic features	High computation time.
NSST+PAPCNN+CSR [99]	MRI-CT, MRI-PET, MRI-SPECT	It shows a better visual quality with detailed edges and texture information.	Vagueness and uncertainties are present in a fused image.
FMI [108]	MRI- CT	Less computation time and the fused image have more complementary data.	CT image information is not clear, which leads to wrong diagnosis.
NPDM [110]	MRI-PET	It represents a clear structure of the tumor region, and the images are available on the axial plane.	This method is not suitable for multiplanar and multi- parametric representations.

2) Calculate the covariance matrix is given by

$$COV(R^1, R^2) = E[(R^1 - \mu_1)(R^2 - \mu_2)] \quad (9)$$

Where E is the expectation vector and average of coefficients are $\mu_1 = \frac{1}{n}\sum_{i=1}^{N} y_i^1$, $\mu_2 = \frac{1}{n}\sum_{i=1}^{N} y_i^2$

3) Compute the Eigen vectors (VC) and Eigenvalues (D) of the covariance matrix from Eq. (**10**)

$$[VC \quad D] = eig(COV) \quad (10)$$

4) Generating normalized weights by *VC*

$$wi_1 = \frac{VC(1)}{\sum\sum VC}, \text{ and } \quad wi_2 = \frac{VC(2)}{\sum\sum VC} \quad (11)$$

5) Finally, fused coefficients are obtained by weighted functions

$$R_F = R^1 \times wi_1 + R^2 \times wi_2 \quad (12)$$

3.2. Energy-based Image Fusion Rule

It is used to extract detailed information from the coefficients of the input images. Examples of energy-based fusion rules are maximum local energy (MLE) [111], and sum-modified-laplacian (SML) [112].

3.2.1. MLE

Depends on the fusion process, the local energy-based fusion rule is applicable for both low and high-frequency coefficients. This fusion rule is used to extract the maximum energy of two input images and produce a fused output image with a 3*3 sliding window. The LE is defined as,

$$LE_\xi = \sum_{x' \in P, y' \in Q} f(x+x', y+y') \bullet LF_\xi^{(0)2}(x+x', y+y') \quad (13)$$

Where *f* is the local filtering operator. *P* and *Q* are the local windows. $\xi \in AorB$ (*A* &*B* are the windows for the two input images).

Local beyond wavelet energy is expressed as

$$LBE_\xi^{(l,k)} = M_1 \times LF_\xi^{(0)2} + M_2 \times LF_\xi^{(0)2} + M_3 \times LF_\xi^{(0)2} \ldots\ldots\ldots\ldots \times M_N \quad (14)$$

Where *M* represents the filtering operators at various directions and *(l, k)* is the scale and direction of the transform.

$$M_1 = \begin{bmatrix} -1 & -1 & -1 \\ 2 & 2 & 2 \\ -1 & -1 & -1 \end{bmatrix} M_2 = \begin{bmatrix} -1 & 2 & -1 \\ -1 & 2 & -1 \\ -1 & 2 & -1 \end{bmatrix} M_1 = \begin{bmatrix} -1 & 0 & -1 \\ 0 & 4 & 0 \\ -1 & 0 & -1 \end{bmatrix}$$

3.2.2. SML

The SML can extract detailed structure information that leads to a better visualization as well as clarity. The SML is defined as:

$$SML(g,h) = \sum_{e=g-a}^{g+a} \sum_{f=h-b}^{h+b} \nabla^2 f(e,f) \quad (15)$$

Where $(2a+1) \times (2b+1)$ are window size, defined around (g,h) and the gradient $\nabla^2 f(e,f)$ is defined as:

$$\nabla^2 f(e,f) = |2f(e,f) - f(e-k,f) - f(e+k,f)| + |2f(e,f) - f(e,f-k) - f(e,f+k)| \quad (16)$$

Here *k* is the step between different coefficients.

3.3. Visualization Based Fusion Rule

The best example of visualization based fusion rule is contrast visibility. It is defined as an amount of difference in intensity values between the image block and the mean value of the block. Contrast visibility is expressed as:

$$CV = \frac{1}{E \times F} \sum_{(e,f) \in B_k} \frac{|f(e,f) - \mu_k|}{\mu_k} \quad (17)$$

Where μ_k, and $E \times F$ are mean and dimensionality of that block B_k, respectively.

3.4. PA-PCNN Based Fusion Rule

The pulse coupled neural network (PCNN) is a biologically inspired neural network that has been extremely used in medical image to extract efficient edge information from high coefficients of input images for better visualization and diagnosis. The PCNN is an iterative procedure and does not require a training process. It is applied in various areas like image classifications, image compression, image fusion, *etc*. The PCNN is a single-layered network with the 2D array input. The conventional PCNN model is a set of various parameters that include amplitudes, linking strengths, and coefficients. The defects in conventional PCNN have a large number of parameters and parameters settings. To overcome this problem, the author [49, 99] proposed PA-PCNN (parameter- adaptive pulse coupled neural network) based fusion rule, which is mathematically described as follows:

$$\begin{aligned} F_{cd}(n) &= S_{cd} \\ L_{cd}(n) &= V_L \sum_{pq} W_{cdpq} Y_{pq}[n-1] \\ U_{cd}(n) &= F_{cd}(n)[1 + \beta L_{cd}(n)] + e^{-\alpha_f} U_{cd}[n-1] \\ \theta_{cd}(n) &= e^{-\alpha_\theta} \theta_{cd}[n-1] + V_E Y_{cd}[n] \\ Y_{cd}(n) &= \begin{cases} 1 & U_{cd}(n) > \theta_{cd}[n-1] \\ 0 & otherwise \end{cases} \end{aligned} \quad (18)$$

Where

$$W_{cdpq} = \begin{bmatrix} 0.5 & 1 & 0.5 \\ 1 & 0 & 1 \\ 0.5 & 1 & 0.5 \end{bmatrix}$$

S_{cd} = Input image, V_L = Amplitude of linking effect, $F_{cd}(n)$ = Feedback input, $L_{cd}(n)$ = Linking input at position (i, j), N = iterations, $U_{cd}(n)$ = Internal activity, β = Linking strength, α_f = Exponential delay function.

3.5. MSF

This fusion rule is used to measure the entire image edge strength in its gradient directions. The mathematical formulation of MSF of an image F is defined as,

$$MSF = \sqrt{RF^2 + CF^2 + SeDF^2 + MaDF^2} \quad \textbf{(19)}$$

$$RF = \sqrt{\frac{1}{G \times H} \sum_{g=1}^{G} \sum_{h=2}^{H} [F(g,h) - F(g,h-1)]^2} \quad \textbf{(20)}$$

$$CF = \sqrt{\frac{1}{G \times H} \sum_{g=2}^{G} \sum_{h=1}^{H} [F(g,h) - F(g-1,h)]^2} \quad \textbf{(21)}$$

$$SeDF = \sqrt{\frac{1}{G \times H} \sum_{g=2}^{G} \sum_{h=1}^{H-1} [F(g,h) - F(g-1,h+1)]^2} \quad \textbf{(22)}$$

$$MaDF = \sqrt{\frac{1}{G \times H} \sum_{g=2}^{G} \sum_{h=2}^{H} [F(g,h) - F(g-1,h-1)]^2} \quad \textbf{(23)}$$

Where *RF, CF, SaDF,* and *MaDF* are the row, column, secondary diagonal, and main diagonal frequencies, respectively.

3.6. IFS Based Cosine Similarity

Let $G = \{\mu_G(c_j), \nu_G(c_j)\}$, and $H = \{\mu_H(c_j), \nu_H(c_j)\}$ be the two IFSs in the universe of discourse C. The cosine similarity function (IFSCS) is used as a fusion rule for the comparison of two IFS's with maximum and minimum selection, and used for medical diagnosis and range belongs to [0-1]. It is described as follows:

$$CS_{IFS}(G,H) \frac{1}{n} \sum_{j=1}^{n} \frac{\mu_G(c_j)\mu_H(c_j) + \nu_G(c_j)\nu_H(c_j)}{\sqrt{\mu_G^2(c_j) + \nu_G^2(c_j)}\sqrt{\mu_H^2(c_j) + \nu_H^2(c_j)}} \quad \textbf{(24)}$$

3.7. Normalized Weighted Sum Based Fusion Rule

The normalized weighted based fusion rule is used to extract the detailed structural information from the image coefficients. Let DC and AC are the detailed and approximation coefficients of the input images G and H, respectively. The mathematical representation of the normalized weighted sum fusion rule is defined as,

$$\begin{aligned} DC^F &= \frac{W_{D1}}{W_{D1} + W_{D2}} \times DC_G + \frac{W_{D2}}{W_{D1} + W_{D2}} \times DC_H \\ AC^F &= \frac{W_{A1}}{W_{A1} + W_{A2}} \times AC_G + \frac{W_{A2}}{W_{A1} + W_{A2}} \times AC_H \end{aligned} \quad \textbf{(25)}$$

$$\begin{aligned} W_{D1} &= \frac{SD^{DC(G)}}{SD^{DC(G)} + SD^{DC(H)}} \\ W_{D2} &= \frac{SD^{DC(H)}}{SD^{DC(G)} + SD^{DC(H)}} \\ W_{A1} &= \frac{SD^{AC(G)}}{SD^{AC(G)} + SD^{AC(H)}} \\ W_{A2} &= \frac{SD^{AC(H)}}{SD^{AC(G)} + SD^{AC(H)}} \end{aligned} \quad \textbf{(26)}$$

where W_{D1}, W_{D2}, W_{A1} & W_{A2} is the standard deviation of the weights of image coefficients G and H.

3.8. Consistency Verification

The consistency verification is a fusion rule used to generate a new decision map for a better-fused image using a majority filter with 7×7 window size. This rule is used to remove wrong focus pixels or errors.

3.9. Phase Congruency (PC)

The PC is used to enhance the features and also to measure the local structures of an image. The PC of an image at (x, y) location is defined as,

$$PC(g,h) = \frac{\sum_i E_{\theta_i}(g,h)}{\varepsilon + \sum_j \sum_i A_{j,\theta_i}(g,h)} \quad \textbf{(27)}$$

where

θ_i = orientation angle at i

A_{j,θ_i} = amplitude of the jth Fourier component and angle θ_i

ε = positive constant

$$E_{\theta_i} = \sqrt{F_{\theta_i}^2(g,h) + H_{\theta_i}^2(g,h)} \quad \textbf{(28)}$$

and the local amplitude at *j* scale is

$$A_{j,\theta_i} = \sqrt{e_{j,\theta_i}^2(g,h) + o_{j,\theta_i}^2(g,h)} \quad \textbf{(29)}$$

$$F_{\theta_i}(g,h) = \sum_j e_{j,\theta_i}(g,h) \quad \textbf{(30)}$$

$$H_{\theta_i}(g,h) = \sum_j o_{j,\theta_i}(g,h) \quad \textbf{(31)}$$

$$[e_{j,\theta_i}(g,h), o_{j,\theta_i}(g,h)] = [I(g,h) * M_j^e, I(g,h) * M_j^o]$$

In Eq (32), M_j^o and M_j^e are the odd and even-symmetric 2-D Log-Gabor filters at scale *j*. **(32)**

4. PERFORMANCE EVALUATION METRICS

Subjective and objective are the two types of methods used for evaluating the quality of a fused image. In subjective evaluation, the fusion quality depends upon the human visual system. The subjective evaluation can be compared with different methods, such as image spatial details, object size, color, *etc*. It has various drawbacks like time consuming, high cost, inconvenience, *etc*. The objective evaluation methods have been proposed to overcome the drawbacks of subjective evaluation. Further, these are classified into two types concerning reference images.

(1) Objective type performance quality metrics with a reference image.

(2) Objective type performance quality metrics without a reference image.

4.1. Objective Type Performance Quality Metrics with a Reference Image

A list of frequently used objective type performance quality metrics with reference images is illustrated in Table **5** and each parameter has its unique characteristics for better visualization and representation. The quality of fusion performance can be calculated by evaluation metrics like discrepancy (D_K) [24], overall performance (OP) [24], cross-correlation (CC) [37], mutual information (MI) [64], similarity measures (SSIM) [65], universal quality index parameter (UQI) [71], mean absolute error (MAE) [71], percentage fit error (PFE) [72], root mean square error (RMSE) [72], peak signal to noise ratio (PSNR) [120], deviation

Table 5. Objective type performance quality metrics with a reference image.

Performance metrics	Description	Equation
D_k	The discrepancy is used to estimate the features of the images. For better fusion performance, the discrepancy value must be small.	$D_k = \frac{1}{E \times F} \sum_{e=1}^{E} \sum_{f=1}^{F} \left\| IMAGE_r(e,f) - IMAGE_f(e,f) \right\|$
OP	It is used to perform the deviation between the average gradient and discrepancy. The value of high OP indicates high fusion quality.	$O.P = \frac{\sum_{k=1}^{3} (D_k - AG_k)}{3}, k = red, green \,\&\, blue.$ Where $AG =$ Average Gradient.
CC	It computes the spectral features of similarity between the reference and fused image. The range is 0-1. The high CC value indicates a high level of fusion.	$CC = \frac{\sum_{g=1}^{G} \sum_{h=1}^{H} \left[(IMAGE_r(g,h) - \overline{IMAGE_r}).(IMAGE_f(g,h) - \overline{IMAGE_f}) \right]}{\sqrt{\sum_{g=1}^{G} \sum_{h=1}^{H} \left[(IMAGE_r(g,h) - (\overline{IMAGE_r}) \right] \sum_{g=1}^{G} \sum_{h=1}^{H} \left[(IMAGE_f(g,h) - \overline{IMAGE_f}) \right]}}$
MI	It is a prominent metric for an indication of dependency levels between fused and reference image/source images. The higher MI value indicates a higher level of fusion.	$MI_{IMAGE_r, IMAGE_f} = \sum_{g=1}^{g} \sum_{h=1}^{h} h_{IMAGE_r, IMAGE_f}(g,h) \log_2 \left[\frac{h_{IMAGE_r, IMAGE_f}(g,h)}{h_{IMAGE_r}(g,h) h_{IMAGE_f}(g,h)} \right]$ $MI = MI_{IMAGE_1 IMAGE_f} + MI_{IMAGE_2 IMAGE_f}$
SSIM	It measures similarities between fused and reference images. SSIM range is [-1, 1]. SSIM is 1 for better fusion.	$SSIM = \frac{[2\mu_{IMAGE_r}\mu_{IMAGE_f} + c_1][2\sigma_{IMAGE_r IMAGE_f} + c_2]}{[\mu^2_{IMAGE_r} + \mu^2_{IMAGE_f} + c_1][\sigma^2_{IMAGE_r} + \sigma^2_{IIMAGE_f} + c_2]}$
UQI	This parameter indicates the level of information transferred from an ideal image to a fused image. The range is [-1, 1]. The higher value of UQI indicates that both images are similar.	$UQI = \frac{4\sigma_{IMAGE_r IMAGE_f}(\mu_{IMAGE_r} + \mu_{IMAGE_f})}{(\sigma^2_{IMAGE_r} + \sigma^2_{IMAGE_f})(\mu^2_{IMAGE_r} + \mu^2_{IMAGE_f})}$
MAE	It is employed to calculate the error between the reference and the fused image.	$MAE = \frac{1}{E \times F} \sum_{e=1}^{E} \sum_{f=1}^{F} \left\| IMAGE_r(e,f) - IMAGE_f(e,f) \right\|$
PFE	The PFE is used to calculate the norm difference between reference and fused image. The lower PFE value indicates both images are ideal.	$PFE = \frac{norm(IMAGE_r - IMAGE_f)}{norm(IMAGE_r)} \times 100$
RMSE	It is used to measure the fusion quality with minimum deviation, *i.e.*, close to 0.	$RMSE = \sqrt{\frac{1}{E \times F} \sum_{e=1}^{E} \sum_{f=1}^{F} \left(IMAGE_r(e,f) - IMAGE_f(e,f) \right)^2}$
PSNR	It represents the probability of intensity levels between fused and reference images. The higher PSNR value indicates that the fused image is good and the range is 0-100	$PSNR = 20 \log_{10} \left[\frac{(255)^2}{\frac{1}{E \times F} \sum_{e=1}^{E} \sum_{f=1}^{F} (IMAGE_r(e,f) - IMAGE_f(e,f))^2} \right]$
DI	This parameter represents the quality of the mixed product of spectral information content. DI should be high for a higher level of fusion.	$DI = \frac{1}{G \times H} \sum_{g=1}^{G} \sum_{h=1}^{H} \frac{\left\| IMAGE_r(g,h) - IMAGE_f(g,h) \right\|}{IMAGE_r(g,h)}$
DIV	DIV is used to identify the variation between fused and the reference image in terms of variance. The lower value of DIV represents high fusion performance.	$DIV = \frac{\sigma_r^2 - \sigma_f^2}{\sigma_r^2}$,
SC	SC is used to calculate the strength of the fused image and the value must be high.	$SC = \frac{\sum_{g=1}^{G} \sum_{h=1}^{H} (IMAGE_r(g,h))^2}{\sum_{g=1}^{G} \sum_{h=1}^{H} (IMAGE_f(g,h))^2}$
AD	It is used to calculate the difference between a fused and a reference image. The lower value represents good fusion quality.	$AD = \frac{1}{E \times F} \sum_{e=1}^{E} \sum_{f=1}^{F} \left(IMAGE_r(e,f) - IMAGE_f(e,f) \right)$
NAE	It is used to calculate the error between the reference and the fused image. The lower value of NAE indicates a good fusion process.	$NAE = \frac{\sum_{g=1}^{G} \sum_{h=1}^{H} \left\| (IMAGE_r(x,y) - IMAGE_f(x,y)) \right\|}{\sum_{g=1}^{G} \sum_{h=1}^{H} (IMAGE_r(x,y))}$

Table 6. Objective type performance quality metrics without a reference image.

Performance Metrics	Description	Equation
SF	SF measures changes in intensity values in a fused image (fused). For good quality fusion performance, the SF value must be large.	$SF=\sqrt{(RF)^2+(CF)^2}$ $RF=\sqrt{\frac{1}{G\times H}\sum_{g=1}^{G}\sum_{h=2}^{H}[fused(g,h)-fused(g,h-1)]^2}$ $CF=\sqrt{\frac{1}{G\times H}\sum_{g=1}^{G}\sum_{h=2}^{H}[fused(g,h)-fused(g-1,h)]^2}$
Petrovic metric ($Q^{AB/F}$)	This metric provides the matching between the edges transmitted in the fusion procedure. For an indication of better fusion, this quality factor should be high.	$Q^{AB/F}=\frac{\sum_{n=1}^{N}\sum_{m=1}^{M}\left(Q^{AF}(n,m)W^{A}(n,m)+Q^{BF}(n,m)W^{B}(n,m)\right)}{\sum_{n=1}^{N}\sum_{m=1}^{M}\left(W^{A}(n,m)+W^{B}(n,m)\right)}$ The range $Q^{AB/F}$ is 0-1.
STD	The standard deviation is to measure the intensity variations in the fused image. STD must be high.	$\sigma=\left\{\frac{1}{G\times H}\sum_{g=1}^{G}\sum_{h=1}^{H}\left[IMAGE_f(g,h)-\mu\right]^2\right\}^{\frac{1}{2}}$
AG	The AG value must be high for better performance of the fusion process.	$AG=\sum_{g=1}^{G}\sum_{h=1}^{H}\frac{\sqrt{[Fu(g,h)-Fu(g+1,h)]^2+[Fu(g,h)-Fu(g,h+1)]^2}}{G\times H}$ Fu= fused image.
E	It measures how much information is in the fused image. The entropy must be high.	$E=-\sum_{l=0}^{L-1}P_l\log P_i$
M	Mean value is used to calculate the average value of the image. For better fusion, the mean value should be high.	$\mu=\frac{1}{G\times H}\sum_{g=1}^{G}\sum_{h=1}^{H}IMAGE_f(g,h)$
FMI	It measures the degree of dependence between the input image and the fused image. The higher FMI value indicates a higher level of fusion.	$FMI=MI_{I_1I_f}+MI_{I_2I_f}$
FF	The fusion factor must be high for better fusion.	$FF=I_{XF}+I_{YF}$
FS	The parameter indicates the degree of symmetry information present in the fused image from the input images. The FS value should be low	$FS=abs\left[\frac{I_{XF}}{I_{XF}+I_{YF}}-0.5\right]$
FI	The fusion index represents the ratio of MI between input images. The FI value should be high.	$FI=\frac{MI_{XF}}{MI_{YF}}$
Piella metrics ($(Q_S(x,y,I_f))$, $(Q_w(x,y,I_f))$, Q_E)	Piella metric is used to estimate the saliency information presented in the fused image and includes edges information. The range of Q (w) is [0-1] and the value is 1 for high fusion performance.	$Q_S(x,y,I_f)=\frac{1}{\lvert w\rvert}\sum_{w\in W}\left(\lambda(w)Q_I(x,I_f\lvert w)\right)+\left((1-\lambda(w))Q_I(y,I_f\lvert w)\right)$ $Q_W(x,y,I_f)=\sum_{w\in W}c(w)\left(\lambda(w)Q_I(x,I_f\lvert w)+(1-\lambda(w))Q_I(y,I_f\lvert w)\right)$ $\lambda(w)=\frac{\sigma_x^{\,2}}{\sigma_x^{\,2}+\sigma_y^{\,2}}$ $c(w)=\max(\sigma_x^{\,2}+\sigma_y^{\,2})$ $Q_E=Q_w(x,y,I_f)\times Q_w(x',y',I_f')^{\alpha}$
SCD	This parameter indicates the level of information which is transmitted from the input images to the fused image and its value is higher for better fusion performance.	$SCD=corr2(fused-img1,img2)+corr2(fused-img2,img1)$
VIS	It measures the clarity of an image for better human perception. The value of visibility high means the fused image is good.	$VIS=\frac{1}{G\times H}\sum_{g=1}^{G}\sum_{h=1}^{H}\frac{\lvert IMAGE_f(g,h)-\mu\rvert}{\mu^{\alpha+1}}$ $\mu=mean,\alpha=visual$

index (DI) [120, 121], difference invariance (DIV) [122], structural content (SC) [123], average difference (AD) [123, 124], and normalized absolute error (NAE) [123, 124],

4.2. Objective Type Performance Quality Metrics Without a Reference Image

This is a highly desirable method to measure the fused image quality without a reference image. A list of frequently used objective type performance quality metrics without a reference image is illustrated in Table **6**. Few metrics are computed with the help of source images and the remaining is related to the fused image for quality measurements, such as spatial frequency (SF) [37], petrovic metric [39], standard deviation (STD) [52], average gradient (AG) [52], entropy (E) [64], mean (M) [72], functional mutual information (FMI) [122], fusion factor (FF) [125, 126], fusion symmetry (FS) [125, 126],fusion index (FI) [126], piella metrics [127], sum of correlation difference (SCD) [128], visibility (VIS) [129].

5. EXPERIMENTAL RESULTS AND DISCUSSION

The performance of medical image fusion methods is evaluated by the benchmark databases, namely, image fusion toolbox [17], whole-brain atlas [18], and another medical image dataset [20]. The database [17, 18, 20] consists of MRI, CT, MRA, PET, and SPECT images with detailed information of the abnormal and normal structure of the brain, and all images are co-aligned as shown in Fig. (**7**). The comparison of existing methods is a typical task because the authors used different multi-modality medical images and evaluation metrics. Various authors suggested different schemes in the literature for medical image fusion, as discussed in section II. The quality evaluation of the fused image is performed in two ways: qualitatively and quantitatively. In this section, a study of various approaches is carried out using subjective and objective type analysis with different medical image applications. The objective analysis of different existing techniques with quality metrics is arranged in a table format, as shown in Table **7**, such as IHS & PCA [22], NSCT [43], IFS [72], SIFS [73], and NSST+PAPCNN [49], and performance quality metrics are mean, standard deviation (STD), average gradient (AG), spatial frequency (SF), entropy (EN), mutual information (MI), and running time.

5.1. MRI-CT Evaluation Group

The subjective type analysis is shown in Fig. (**8**). Fig. (**8a** and **b**) are multi-modality images, which provide soft and hard tissue information. Fig. (**8c**) shows the complementary information which is not clearly visible. Fig. (**8d**) represents a degraded fused image, which represents MRI

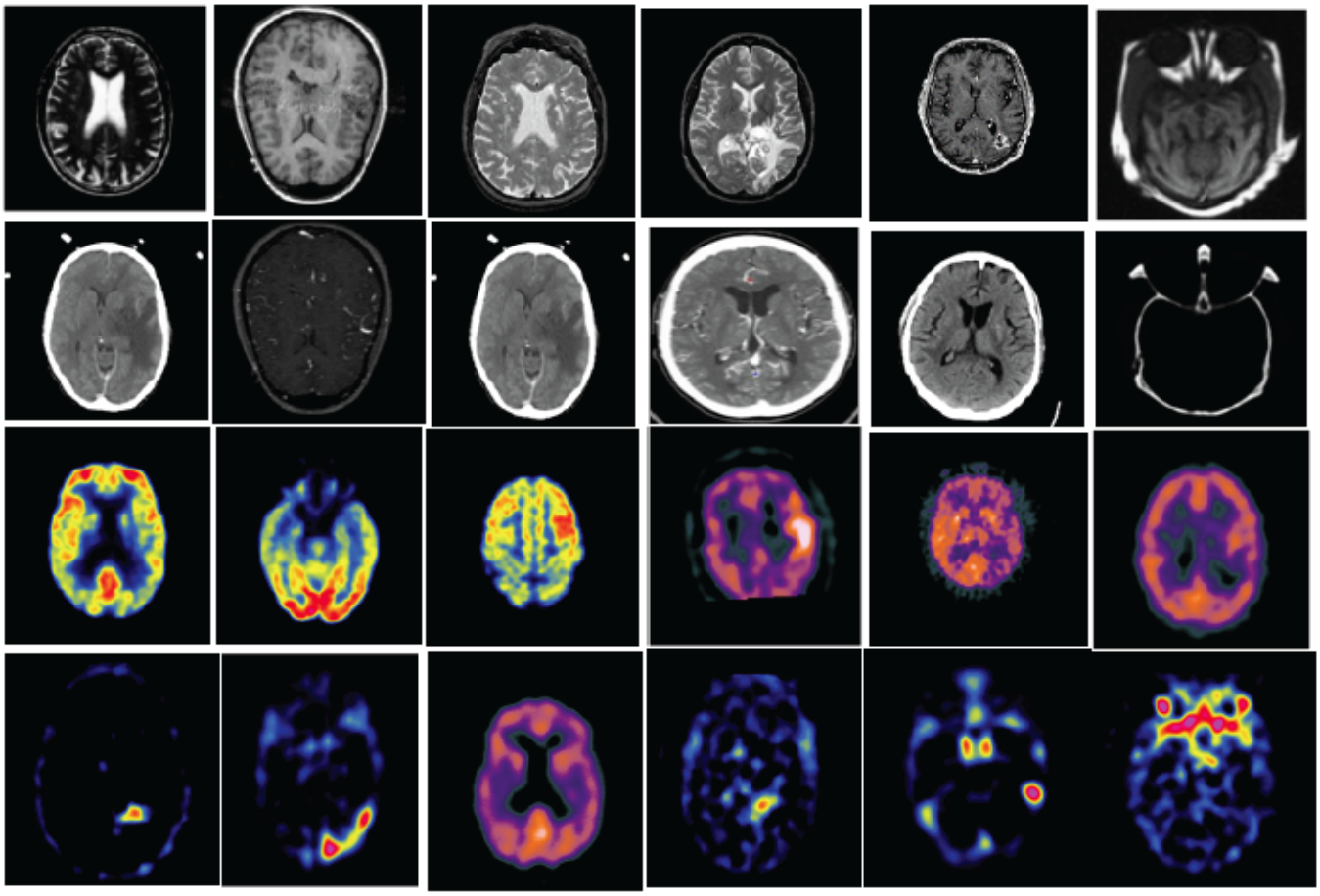

Fig. (7). Multi modal medical image fusion dataset examples for fusion process [17-18, 20]. (*A higher resolution / colour version of this figure is available in the electronic copy of the article*).

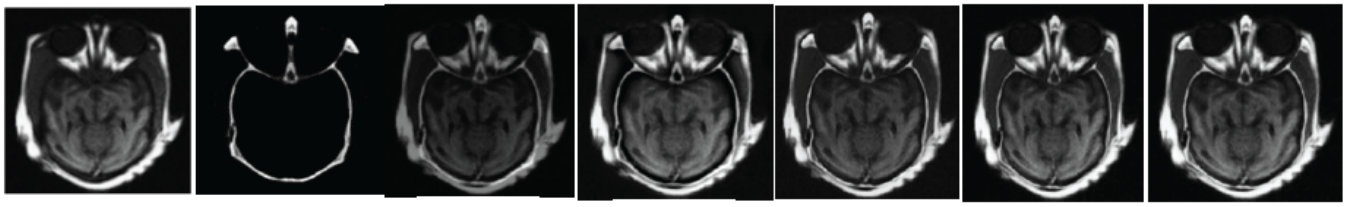

Fig. (8). Experimental results for MRI-CT images. (**a**) MRI image, (**b**) CT image, (**c**) IHS & PCA, (**d**) NSCT, (**e**) IFS, (**f**) SIFS, (**g**) NSST+PAPCNN. (*A higher resolution / colour version of this figure is available in the electronic copy of the article*).

information. Fig. (**8e**) represents low quality fused image. The detailed edges and enhanced fused image areas shown in Fig. (**8f-g**).

In objective type analysis of MRI-CT fusion methods, the IFS based medical image fusion method produced the highest value for mutual information (MI), 5.8989, which indicates the transfer of the high information from a source image into the fused image. The SIFS gives the highest values of 62.7349 for standard deviation (STD), and 18.9252 for spatial frequency (SF) with low computation time (0.4429 sec); it indicates detailed texture information present in a fused image. NSST+PAPCNN based medical image fusion method gives the highest values of 6.5927 for entropy (E), and 57.9767 for mean, which indicates the fused image has more information with good resolution. NSCT based fusion method gives highest value of 7.3979 for average gradient, means fused image has more detailed information.

5.2. T1-weighted MR - MRA Evaluation Group

The subjective type analysis is shown in Fig. (**9**). Fig. (**9a** & **b**) shows multi-modality images, which provide information of soft lesions. Fig. (**9c**) shows the degraded fused image. Fig. (**9d-e**) represents a detailed structured fused image, which represents lesion location has clear visibility. Fig. (**9f**) represents more texture information. The detailed edges and enhanced fused image areas are shown in Fig. (**9g**). In objective type analysis of T1-weighted MR -MRA fusion methods, the SIFS based medical image fusion method produced the highest values of 67.8497 for mean, 68.9038 for STD, and 4.9515 for MI with low computation time (0.5032 sec), which indicates good contrast in a fused image. NSCT based fusion method gives the highest value of 10.1804 for AG, and 26.2009 for SF, it represents detailed texture information present in a fused image. NSST+PAPCNN fusion method attains a higher value for EN, 6.6468, which represents a fused image is more informative.

5.3. MRI-PET Evaluation Group

Table **7** shows the Glioma disease of MRI-PET medical image fusion based on various existing methods and quality metrics. The subjective type analysis of MRI-PET image fusion is shown in Fig. (**10**). Fig. (**10a** and **b**) shows the multi-modality images with soft tissue and functionality information. Fig. (**10c**) shows the degraded fused image, which is not suitable for diagnosis. Low contrast fused image is shown in Fig. (**10d**). The detailed complementary information present in a fused image is shown in Fig. (**10e**). Fig. (**10f**) images show the enhanced fused image, which is used to identify the tumour region efficiently with better diagnosis. Lastly, a low enhanced fused image is observed in Fig. (**10g**).

In objective type analysis of MRI-PET medical image fusion methods, the SIFS based medical image fusion method produced the highest values of 29.9189 for mean, and 58.7795 for STD with low computation time (0.4612 sec), which indicates a well enhanced fused image. NSCT based fusion method gives the highest value of 6.9015 for AG, and 28.317 for SF, which indicates detailed edge information is present in a fused image. NSST+PAPCNN fusion method attains higher values of 2.9734 for EN, and 3.7551 for MI; it represents more information is transferred from source images.

5.4. MRI-Spect Evaluation Group

The subjective type analysis of MRI-SPECT image fusion is shown in Fig. (**11**). Fig. (**11a** and **b**) shows multimodality images, that provide soft tissue and blood flow information. Fig. (**11c**) shows the degraded fused image. The more complementary information present in a fused image is shown in Fig. (**11d**). Fig. (**11e**) represents quality fused images with a clear structure. Fig. (**11f**) represents better edge information, and a better visualized fused image. Lastly, detailed edge and structure information is present in the fused image, as shown in Fig. (**11g**).

In objective type analysis of MRI-SPECT medical image fusion methods, the NSCT based fusion method attains a higher value for SF, 21.6799, which represents good texture information. SIFS based fusion method gives the highest values of 47.8104 for Mean, 62.4093 for STD, 5.0656 for EN, and 5.1860 for MI with low comutation time (0.4688 sec), which indicates more detailed textural information is present in a fused image. NSST+PAPCNN based fusion method produced the highest value of 7.8165 AG, which indicates the fused image is well structured.

CONCLUSION

The Multimodal Medical Image Fusion (MMIF) plays a tremendous role in the present bio-medical research. The purpose of MMIF is to enhance the image quality in all aspects without artifacts and color distortions. In this paper, we present a detailed review of multi-modal medical images, fusion methods, image fusion rules, quality evaluation metrics, and finally, a comparison of all existing techniques, which will lead to future research.

Many of the researchers proposed different fusion methods, which are the modified version of existing ones, and

Table 7. Comparison of various existing methods with different datasets.

Datasets	Fusion Techniques	Mean	STD	AG	SF	EN	MI	Running time (Sec)
MRI-CT	IHS & PCA	28.1525	29.7206	3.9726	12.5567	4.2321	5.3126	1.25
	NSCT	55.7727	60.0306	**7.3979**	18.6704	6.5463	5.3827	10.81
	IFS	56.2292	60.8907	6.9227	17.6850	6.2152	**5.8989**	0.6712
	SIFS	57.7266	**62.7349**	7.2502	**18.9252**	6.2628	5.8886	**0.4429**
	NSST+PAPCNN	**57.9767**	61.5506	6.9023	17.2323	**6.5927**	5.3858	25.81
T1-weighted MR & MRA	IHS & PCA	11.3707	11.3495	4.6097	14.0983	4.2577	4.8555	1.72
	NSCT	66.3808	67.2207	**10.1804**	**26.2009**	6.3323	4.7910	11.64
	IFS	59.33	62.4487	9.3827	25.3612	4.7583	4.8549	0.6435
	SIFS	**67.8497**	**68.9038**	9.8371	24.2625	4.9037	**4.9515**	**0.5032**
	NSST+PAPCNN	66.6708	68.2066	9.0896	25.0663	**6.6468**	3.8854	27.85
MRI-PET	IHS & PCA	15.8455	15.9531	4.0350	140582	2.9667	3.3096	1.71
	NSCT	17.8876	41.9828	**6.9015**	**28.3187**	2.5733	3.5712	18.99
	IFS	27.9612	55.7105	5.2412	23.2345	2.9183	3.7193	0.5912
	SIFS	**29.9189**	**58.7795**	5.6967	25.2336	2.9482	3.7081	**0.4612**
	NSST+PAPCNN	17.9179	41.9672	6.8974	28.3178	**2.9734**	**3.7551**	25.42
MRI-SPECT	IHS & PCA	14.2144	17.5271	3.2092	14.0588	2.4556	3.9638	1.67
	NSCT	42.0009	58.6003	7.8145	**21.6799**	4.5954	4.9348	18.25
	IFS	40.2415	56.1923	6.5123	18.9745	4.6669	5.1288	0.6754
	SIFS	**47.8104**	**62.4093**	4.9652	14.7244	**5.0656**	**5.1860**	**0.4688**
	NSST+PAPCNN	42.0021	58.6007	**7.8165**	21.5805	4.5954	4.9211	24.22

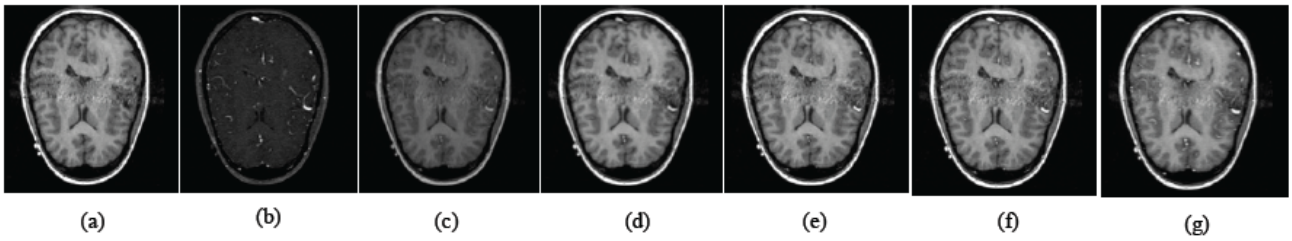

Fig. (9). Experimental results for T1- weighted MRI-MRA images. (**a**) T1-weighted MR image, (**b**) MRA image, (**c**)IHS & PCA, (**d**) NSCT, (**e**) IFS, (**f**) SIFS, (**g**) NSST+PAPCNN. (*A higher resolution / colour version of this figure is available in the electronic copy of the article*).

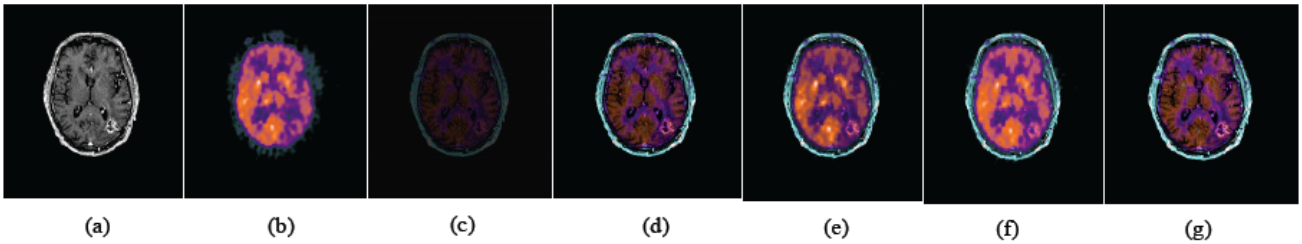

Fig. (10). Experimental results for T1- weighted MRI-MRA images. (**a**) T1-weighted MR image, (**b**) MRA image, (**c**) IHS & PCA, (**d**) NSCT, (**e**) IFS, (**f**) SIFS, (**g**) NSST+PAPCNN. (*A higher resolution / colour version of this figure is available in the electronic copy of the article*).

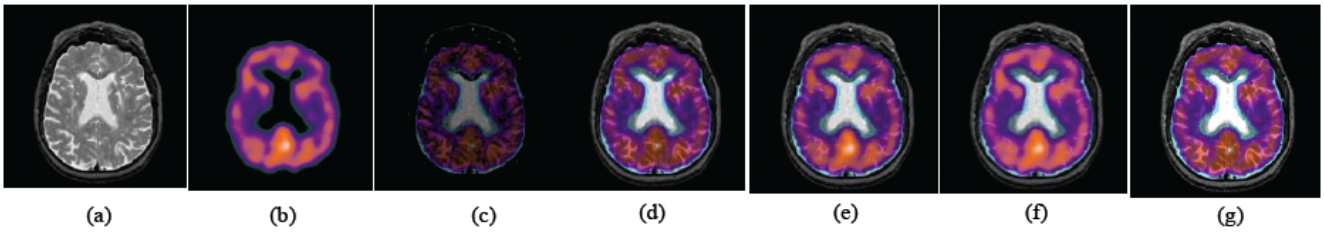

Fig. (11). Experimental results for T1- weighted MRI-MRA images. (**a**) T1-weighted MR image, (**b**) MRA image, (**c**) IHS & PCA, (**d**) NSCT, (**e**) IFS, (**f**) SIFS, (**g**) NSST+PAPCNN. (*A higher resolution / colour version of this figure is available in the electronic copy of the article*).

they are not sufficient enough to support the medical diagnosis completely. The multi-resolution algorithms are more helpful for medical image fusion to extract the features at various scales and directions to satisfy the shift-invariant property. The scale and orientations are important criteria in medical image fusion. Many algorithms are proposed related to scales and orientations. Sparse representation (SR) and saliency-based fusion methods provide better visualization and edge enhancement, respectively. Deep learning is a new era in the medical field for better diagnosis, but it faces various difficulties such as the complexity of the deep learning network framework, lack of training datasets, and high expense. Finally, fuzzy set based fusion methods provide enhanced fused images without uncertainties and vagueness. It is difficult to conclude that a single fusion method is good in all aspects. Each methodology has its advantages and drawbacks, which are emphasized in this review.

The image fusion rules are significantly used to extract the feature to improve the quality of an image. The standard image quality evaluation metrics are well discussed in this paper to decide the quality of fusion performance. So the image fusion methods, fusion rules, and performance quality metrics play an important role in enhancing the quality of the image. However, the challenging tasks in medical imaging synthesis are noise, complexity, high cost, lack of sufficient features, *etc*. In the future, more sophisticated algorithms must be developed to overcome the above-mentioned problems. Those modalities are helpful to the physician for better perception and identification of the diseases.

CONSENT FOR PUBLICATION

Not applicable.

FUNDING

None.

CONFLICT OF INTEREST

The authors declare no conflict of interest, financial or otherwise.

ACKNOWLEDGEMENTS

Declared none.

REFERENCES

[1] Du J, Li W, Lu K, Xiao B. An overview of multi-modal medical image fusion. Neurocomputing 2016; 215: 3-20. http://dx.doi.org/10.1016/j.neucom.2015.07.160

[2] Azam MA, Khan KB, Ahmad M, Mazzara M. Multimodal medical image registration and fusion for quality enhancement. Comput Mater Cont 2021; 68(2021): 821-40.

[3] Kaur H, Koundal D, Kadyan V. Image fusion techniques: A survey. Arch Comput Methods Eng 2021; 28(7): 4425-47. http://dx.doi.org/10.1007/s11831-021-09540-7 PMID: 33519179

[4] Hermessi H, Mourali O, Zagrouba E. Multimodal medical image fusion review: Theoretical background and recent advances. Signal Process 2021; 183: 108036. http://dx.doi.org/10.1016/j.sigpro.2021.108036

[5] Tawfik N, Elnemr HA, Fakhr M, Dessouky MI, El-Samie A, Fathi E. Survey study of multimodality medical image fusion methods. Multimedia Tools Appl 2021; 80(4): 6369-96. http://dx.doi.org/10.1007/s11042-020-08834-5

[6] Swathi PS, Sheethal MS, Paul V. Survey on multimodal medical image fusion techniques. Int J Sci Eng Comput Technol 2016; 6(1): 33.

[7] Li Y, Zhao J, Lv Z, Li J. Medical image fusion method by deep learning. Int J Cogn Comput Eng 2021; 2: 21-9. http://dx.doi.org/10.1016/j.ijcce.2020.12.004

[8] Azam MA, Khan KB, Salahuddin S, *et al.* A review on multimodal medical image fusion: Compendious analysis of medical modalities, multimodal databases, fusion techniques and quality metrics. Comput Biol Med 2022; 144: 105253. http://dx.doi.org/10.1016/j.compbiomed.2022.105253 PMID: 35245696

[9] Heba M, Rabaieb ES, Elrahmana WA, Faragallahc OS, El-Samieb FE. Medical image fusion: A literature review present solutions and future directions. Minufiya J Electron Eng Res 2017; 26(2): 1-62.

[10] Ramandeep RK. Review on different aspects of image fusion for medical imaging. Int J Sci Res 2014; 3(5): 1887-9.

[11] James AP, Dasarathy BV. Medical image fusion: A survey of the state of the art. Inf Fusion 2014; 19: 4-19. http://dx.doi.org/10.1016/j.inffus.2013.12.002

[12] Huang B, Yang F, Yin M, Mo X, Zhong C. A review of multimodal medical image fusion techniques. Comput Math Methods Med 2020; 2020: 8279342. http://dx.doi.org/10.1155/2020/8279342 PMID: 32377226

[13] El-Gamal FE, Elmogy M, Atwan A. Current trends in medical image registration and fusion. Egyptian Inform J 2016; 17(1): 99-124. http://dx.doi.org/10.1016/j.eij.2015.09.002

[14] Tirupal T, Mohan BC, Kumar SS. Multimodal medical image fusion techniques–A review. Curr Signal Transduct Ther 2021; 16(2): 142-63. http://dx.doi.org/10.2174/1574362415666200226103116

[15] Meher B, Agrawal S, Panda R, Abraham A. A survey on region based image fusion methods. Inf Fusion 2019; 48: 119-32. http://dx.doi.org/10.1016/j.inffus.2018.07.010

[16] Narsaiah MN, Vathsal S, Reddy DV. A survey on image fusion requirements, techniques, evaluation metrics, and its applications. Int J Eng Technol 2018; 7(2.20): 260-6.

[17] Rockinger O. Image fusion toolbox for Matlab. Technical report, Metapix 1999. Available from: http://www. metapix. de/toolbox. htm

[18] Johnson KA, Becker JA. The Whole Brain Atlas. Available from: http://www.med.harvard.edu/AANLIB/home.html

[19] Available from: https://wiki.cancerimagingarchive.net/pages/viewpage.action?pageId=70224216

[20] Durga Prasad Bavirisetti. Medical Imaging datasets. Available from: https://sites.google.com/view/durgaprasadbavirisetti/datasets. (Accessed on: 18-08-2020).

[21] Available from: https://www.google.com/search?q=Fusion+of+vibro-acoustography+images+and+X-ray+mammography&client=firefox-b-d&source=lnms&tbm=isch&sa=X&ved=2ahUKEwiE3Y7QwvL2AhX2xTgGHclrB1sQ_AUoAXoECAEQAw&biw=1366&bih=643&dpr=1

[22] He C, Liu Q, Li H, Wang H. Multimodal medical image fusion based on IHS and PCA. Proc Eng 2010; 7: 280-5. http://dx.doi.org/10.1016/j.proeng.2010.11.045

[23] Daneshvar S, Ghassemian H. MRI and PET image fusion by combining IHS and retina-inspired models. Inf Fusion 2010; 11(2): 114-23. http://dx.doi.org/10.1016/j.inffus.2009.05.003

[24] Haddadpour M, Daneshvar S, Seyedarabi H. PET and MRI image fusion based on combination of 2-D Hilbert transform and IHS method. Biomed J 2017; 40(4): 219-25. http://dx.doi.org/10.1016/j.bj.2017.05.002 PMID: 28918910

[25] Du J, Li W, Xiao B, Nawaz Q. Union Laplacian pyramid with multiple features for medical image fusion. Neurocomputing 2016; 194: 326-39. http://dx.doi.org/10.1016/j.neucom.2016.02.047

[26] Krishnamoorthy S, Soman KP. Implementation and comparative study of image fusion algorithms. Int J Comput Appl 2010; 9(2): 25-35.

[27] Yang Y, Park DS, Huang S, Rao N. Medical image fusion *via* an effective wavelet-based approach. EURASIP J Adv Signal Process 2010; 2010: 1-3.

[28] Singh R, Khare A. Multiscale medical image fusion in wavelet domain. Sci World J 2013; 2013: 521034. http://dx.doi.org/10.1155/2013/521034

[29] Suraj AA, Francis M, Kavya TS, Nirmal TM. Discrete wavelet transform based image fusion and de-noising in FPGA. J Electrical Sys Inform Technol 2014; 1(1): 72-81. http://dx.doi.org/10.1016/j.jesit.2014.03.006

[30] Chandra SJ, Babu AN, Rao GS, *et al.* Medical fusion image using wavelet transformation. Int J Innov Technol Explor Eng 2019; 8(8): 1864-6.

[31] Gomathi PS, Kalaavathi B. Medical image fusion based on redundant wavelet transform and morphological processing. Int J Comput Inform Eng 2014; 8(6): 1018-22.

[32] Yadav HN. Multimodal medical image fusion for computer aided diagnosis. Comput Trendz 2015; 5(1 & 2): 21-5.

[33] Wang HH. A new multiwavelet-based approach to image fusion. J Math Imaging Vis 2004; 21(2): 177-92. http://dx.doi.org/10.1023/B:JMIV.0000035181.00093.e3

[34] Wang X, Shen Y, Zhou Z, Fang L. An image fusion algorithm based on lifting wavelet transform. J Opt 2015; 17(5): 055702. http://dx.doi.org/10.1088/2040-8978/17/5/055702

[35] El-Hoseny HM, Abd El-Rahman W, El-Rabaie ES, Abd El-Samie FE, Faragallah OS. An efficient DT-CWT medical image fusion system based on modified central force optimization and histogram matching. Infrared Phys Technol 2018; 94: 223-31. http://dx.doi.org/10.1016/j.infrared.2018.09.003

[36] Alipour SHM, Houshyari M, Mostaar A. A novel algorithm for PET and MRI fusion based on digital curvelet transform *via* extracting lesions on both images. Electron Physician 2017; 9(7): 4872-9. http://dx.doi.org/10.19082/4872 PMID: 28894548

[37] Yang L, Guo BL, Ni W. Multimodality medical image fusion based on multiscale geometric analysis of contourlet transform. Neurocomputing 2008; 72(1-3): 203-11. http://dx.doi.org/10.1016/j.neucom.2008.02.025

[38] Huang H, Feng XA, Jiang J. Medical image fusion algorithm based on nonlinear approximation of contourlet transform and regional features. J Electr Comput Eng 2017; 2017: 6807473. http://dx.doi.org/10.1155/2017/6807473

[39] Bhatnagar G, Wu QJ, Liu Z. Directive contrast based multimodal medical image fusion in NSCT domain. IEEE Trans Multimed 2013; 15(5): 1014-24. http://dx.doi.org/10.1109/TMM.2013.2244870

[40] Yang G, Li M, Chen L, Yu J. The nonsubsampled contourlet transform based statistical medical image fusion using generalized Gaussian density. Comput Math Methods Med 2015; 2015: 262819. http://dx.doi.org/10.1155/2015/262819 PMID: 26557871

[41] Bhatnagar G, Wu QJ, Liu Z. A new contrast based multimodal medical image fusion framework. Neurocomputing 2015; 157: 143-52. http://dx.doi.org/10.1016/j.neucom.2015.01.025

[42] Gomathi PS, Kalaavathi B. Multimodal medical image fusion in non-subsampled contourlet transform domain. Circuits Sys 2016; 7(08): 1598. http://dx.doi.org/10.4236/cs.2016.78139

[43] Zhu Z, Zheng M, Qi G, Wang D, Xiang Y. A phase congruency and local Laplacian energy based multi-modality medical image fusion method in NSCT domain. IEEE Access 2019; 7: 20811-24. http://dx.doi.org/10.1109/ACCESS.2019.2898111

[44] Miao QG, Shi C, Xu PF, Yang M, Shi YB. A novel algorithm of image fusion using shearlets. Opt Commun 2011; 284(6): 1540-7. http://dx.doi.org/10.1016/j.optcom.2010.11.048

[45] Ahmed N. Medical image fusion based on shearlets and human feature visibility. Int J Comput Appl 2015; 125(12): 7-12.

[46] Biswas B, Sen BK. Color PET-MRI medical image fusion combining matching regional spectrum in shearlet domain. Int J Image Graph 2019; 19(01): 1950004. http://dx.doi.org/10.1142/S0219467819500049

[47] Xiaoxue X, Fucheng C, Weiwei S, Fu L. Multi-modal medical image fusion based on non-subsampled Shearlet Transform. Int J Signal Process Image Process Pattern Recogn 2015; 8(2): 41-8. http://dx.doi.org/10.14257/ijsip.2015.8.2.05

[48] Singh S, Anand RS. Multimodal neurological image fusion based on adaptive biological inspired neural model in nonsubsampled shearlet domain. Int J Imaging Syst Technol 2019; 29(1): 50-64. http://dx.doi.org/10.1002/ima.22294

[49] Yin M, Liu X, Liu Y, Chen X. Medical image fusion with parameter-adaptive pulse coupled neural network in nonsubsampled shearlet transform domain. IEEE Trans Instrum Meas 2018; 68(1): 49-64. http://dx.doi.org/10.1109/TIM.2018.2838778

[50] Li S, Yin H. Multimodal image fusion with joint sparsity model. Opt Eng 2011; 50(6): 067007. http://dx.doi.org/10.1117/1.3584840

[51] Shreyamsha Kumar BK. Image fusion based on pixel significance using cross bilateral filter. Signal Image Video Process 2015; 9(5): 1193-204. http://dx.doi.org/10.1007/s11760-013-0556-9

[52] Bavirisetti DP, Kollu V, Gang X, Dhuli R. Fusion of MRI and CT images using guided image filter and image statistics. Int J Imaging Syst Technol 2017; 27(3): 227-37. http://dx.doi.org/10.1002/ima.22228

[53] Bavirisetti DP, Xiao G, Zhao J, Dhuli R, Liu G. Multi-scale guided image and video fusion: A fast and efficient approach. Circuits Syst Signal Process 2019; 38(12): 5576-605. http://dx.doi.org/10.1007/s00034-019-01131-z

[54] Jiang Y, Wang M. Image fusion using multiscale edge-preserving decomposition based on weighted least squares filter. IET Image Process 2014; 8(3): 183-90. http://dx.doi.org/10.1049/iet-ipr.2013.0429

[55] Jian L, Yang X, Zhou Z, Zhou K, Liu K. Multi-scale image fusion through rolling guidance filter. Future Gener Comput Syst 2018; 83: 310-25. http://dx.doi.org/10.1016/j.future.2018.01.039

[56] Zhang Y, Li D, Zhang R, Cui Y. Sparse features with fast guided filtering for medical image fusion. J Med Imaging Health Inform 2020; 10(5): 1195-204. http://dx.doi.org/10.1166/jmihi.2020.2998

[57] Yadav SS, Jadhav SM. Deep convolutional neural network based medical image classification for disease diagnosis. J Big Data 2019; 6(1): 1-8. http://dx.doi.org/10.1186/s40537-019-0276-2

[58] Kermany DS, Goldbaum M, Cai W, *et al.* Identifying medical diagnoses and treatable diseases by image-based deep learning. Cell 2018; 172(5): 1122-1131.e9. http://dx.doi.org/10.1016/j.cell.2018.02.010 PMID: 29474911

[59] Hesamian MH, Jia W, He X, Kennedy P. Deep learning techniques for medical image segmentation: Achievements and challenges. J Digit Imaging 2019; 32(4): 582-96. http://dx.doi.org/10.1007/s10278-019-00227-x PMID: 31144149

[60] Zhou T, Ruan S, Canu S. A review: Deep learning for medical image segmentation using multi-modality fusion. Array 2019; 3: 100004. http://dx.doi.org/10.1016/j.array.2019.100004

[61] Chen C, Qin C, Qiu H, *et al.* Deep learning for cardiac image segmentation: A review. Front Cardiovasc Med 2020; 7: 25. http://dx.doi.org/10.3389/fcvm.2020.00025 PMID: 32195270

[62] Liu Y, Chen X, Peng H, Wang Z. Multi-focus image fusion with a deep convolutional neural network. Inf Fusion 2017; 36: 191-207. http://dx.doi.org/10.1016/j.inffus.2016.12.001

[63] Hermessi H, Mourali O, Zagrouba E. Convolutional neural network-based multimodal image fusion *via* similarity learning in the shearlet domain. Neural Comput Appl 2018; 30(7): 2029-45. http://dx.doi.org/10.1007/s00521-018-3441-1

[64] Hou R, Zhou D, Nie R, Liu D, Ruan X. Brain CT and MRI medical image fusion using convolutional neural networks and a dual-channel spiking cortical model. Med Biol Eng Comput 2019; 57(4): 887-900. http://dx.doi.org/10.1007/s11517-018-1935-8 PMID: 30471068

[65] Wang M, Liu X, Jin H. A generative image fusion approach based on supervised deep convolution network driven by weighted gradient flow. Image Vis Comput 2019; 86: 1-6. http://dx.doi.org/10.1016/j.imavis.2019.02.011

[66] Haskins G, Kruger U, Yan P. Deep learning in medical image registration: A survey. Mach Vis Appl 2020; 31(1): 1-8. http://dx.doi.org/10.1007/s00138-020-01060-x

[67] Ismail WZ, Sim KS. Contrast enhancement dynamic histogram equalization for medical image processing application. Int J Imaging Syst Technol 2011; 21(3): 280-9. http://dx.doi.org/10.1002/ima.20295

[68] Maini R, Aggarwal H. A comprehensive review of image enhancement techniques. arXiv 2010; 2010: 1003.4053.

[69] Lotfi Zadeh A. Fuzzy set. Inf Control 1965; 8(3): 338-53. http://dx.doi.org/10.1016/S0019-9958(65)90241-X

[70] Atanasov KT. Intuitionistic fuzzy sets. Fuzzy Sets Syst 1986; 20(1): 87-96. http://dx.doi.org/10.1016/S0165-0114(86)80034-3

[71] Sanjay AR, Soundrapandiyan R, Karuppiah M, Ganapathy R CT. International Journal of Intelligent Engineering and Systems 2017; 10(3): 355-62. http://dx.doi.org/10.22266/ijies2017.0630.40

[72] Balasubramaniam P, Ananthi VP. Image fusion using intuitionistic fuzzy sets. Inf Fusion 2014; 20: 21-30. http://dx.doi.org/10.1016/j.inffus.2013.10.011

[73] Aysha S, Tirupal T. Image fusion of medical images based on Fuzzy set. Elixir Digital Processing 2016; 96: 41225-8.

[74] Soundrapandiyan R, Haldar R, Purushotham S, Pillai A. Multimodality medical image fusion using block based intuitionistic fuzzy sets. IIOAB J 2016; 7(5): 85-94.

[75] Soundrapandiyan R, Karuppiah M, Kumari S, Kumar Tyagi S, Wu F, Jung KH. An efficient DWT and intuitionistic fuzzy based multimodality medical image fusion. Int J Imaging Syst Technol 2017; 27(2): 118-32. http://dx.doi.org/10.1002/ima.22216

[76] Kumar M, Kaur A. Amita. Improved image fusion of colored and grayscale medical images based on intuitionistic fuzzy sets. Fuzzy Inform Eng 2018; 10(2): 295-306. http://dx.doi.org/10.1080/16168658.2018.1517980

[77] Tirupal T, Mohan BC, Kumar SS. Multimodal medical image fusion based on Sugeno's intuitionistic fuzzy sets. ETRI J 2017; 39(2): 173-80. http://dx.doi.org/10.4218/etrij.17.0116.0568

[78] Tirupal T, Chandra Mohan B, Srinivas Kumar S. Multimodal medical image fusion based on yager's intuitionistic fuzzy sets. Iran J Fuzzy Sys 2019; 16(1): 33-48.

[79] Agarwal J, Bedi SS. Implementation of hybrid image fusion technique for feature enhancement in medical diagnosis. Human-centric Comput Inform Sci 2015; 5(1): 1-7. http://dx.doi.org/10.1186/s13673-014-0020-z

[80] Dai Y, Zhou Z, Xu L. The application of multi-modality medical image fusion based method to cerebral infarction. EURASIP J Image Video Process 2017; 2017(1): 1-6. http://dx.doi.org/10.1186/s13640-017-0204-3

[81] Zong JJ, Qiu TS. Medical image fusion based on sparse representation of classified image patches. Biomed Signal Process Control 2017; 34: 195-205. http://dx.doi.org/10.1016/j.bspc.2017.02.005

[82] Aktar MN, Lambert AJ, Pickering M. An automatic fusion algorithm for multi-modal medical images. Comput Methods Biomech Biomed Eng Imaging Vis 2018; 6(5): 584-98. http://dx.doi.org/10.1080/21681163.2017.1304244

[83] Daniel E, Anitha J, Kamaleshwaran KK, Rani I. Optimum spectrum mask based medical image fusion using Gray Wolf Optimization. Biomed Signal Process Control 2017; 34: 36-43. http://dx.doi.org/10.1016/j.bspc.2017.01.003

[84] Xia J, Chen Y, Chen A, Chen Y. Medical image fusion based on sparse representation and PCNN in NSCT domain. Comput Math Methods Med 2018; 2018: 2806047. http://dx.doi.org/10.1155/2018/2806047 PMID: 29991960

[85] Daniel E. Optimum wavelet-based homomorphic medical image fusion using hybrid genetic–grey wolf optimization algorithm. IEEE Sens J 2018; 18(16): 6804-11. http://dx.doi.org/10.1109/JSEN.2018.2822712

[86] Tan L, Yu X. Medical image fusion based on fast finite shearlet transform and sparse representation. Comput Math Methods Med 2019; 2019: 3503267. http://dx.doi.org/10.1155/2019/3503267 PMID: 30944576

[87] Hassan M, Murtza I, Zafar Khan MA, Tahir SF, Fahad LG. Neuro-wavelet based intelligent medical image fusion. Int J Imaging Syst Technol 2019; 29(4): 633-44. http://dx.doi.org/10.1002/ima.22347

[88] Ramlal SD, Sachdeva J, Ahuja CK, Khandelwal N. An improved multimodal medical image fusion scheme based on hybrid combination of nonsubsampled contourlet transform and stationary wavelet transform. Int J Imaging Syst Technol 2019; 29(2): 146-60. http://dx.doi.org/10.1002/ima.22310

[89] Rajalingam B, Priya R, Bhavani R. Medical image fusion based on hybrid algorithms for neuro cysticercosis and neoplastic disease analysis. IMCMS 2019; 2019: 15. http://dx.doi.org/10.26782/jmcms.2019.08.00015

[90] Huang C, Tian G, Lan Y, *et al.* A new pulse coupled neural network (PCNN) for brain medical image fusion empowered by shuffled frog leaping algorithm. Front Neurosci 2019; 13: 210. http://dx.doi.org/10.3389/fnins.2019.00210 PMID: 30949018

[91] Li J, Peng Y, Song M, Liu L. Image fusion based on guided filter and online robust dictionary learning. Infrared Phys Technol 2020; 105: 103171. http://dx.doi.org/10.1016/j.infrared.2019.103171

[92] El-Hoseny HM, Abd El-Rahman W, El-Shafai W, *et al.* Efficient multi-scale non-sub-sampled shearlet fusion system based on modified central force optimization and contrast enhancement. Infrared Phys Technol 2019; 102: 102975. http://dx.doi.org/10.1016/j.infrared.2019.102975

[93] Hu Q, Hu S, Zhang F. Multi-modality medical image fusion based on separable dictionary learning and Gabor filtering. Signal Process Image Commun 2020; 83: 115758. http://dx.doi.org/10.1016/j.image.2019.115758

[94] Parvathy VS, Pothiraj S. Multi-modality medical image fusion using hybridization of binary crow search optimization. Health Care Manage Sci 2020; 23(4): 661-9. http://dx.doi.org/10.1007/s10729-019-09492-2 PMID: 31292844

[95] Xu L, Si Y, Jiang S, Sun Y, Ebrahimian H. Medical image fusion using a modified shark smell optimization algorithm and hybrid wavelet-homomorphic filter. Biomed Signal Process Control 2020; 59: 101885. http://dx.doi.org/10.1016/j.bspc.2020.101885

[96] Liu Y, Zhou D, Nie R, *et al.* Robust spiking cortical model and total-variational decomposition for multimodal medical image fusion. Biomed Signal Process Control 2020; 61: 101996. http://dx.doi.org/10.1016/j.bspc.2020.101996

[97] Maqsood S, Javed U. Multi-modal medical image fusion based on two-scale image decomposition and sparse representation. Biomed Signal Process Control 2020; 57: 101810. http://dx.doi.org/10.1016/j.bspc.2019.101810

[98] Ding Z, Zhou D, Nie R, Hou R, Liu Y. Brain medical image fusion based on dual-branch CNNs in NSST domain. BioMed Res Int 2020; 2020: 6265708. http://dx.doi.org/10.1155/2020/6265708 PMID: 32352003

[99] Xia J, Lu Y, Tan L. Research of multimodal medical image fusion based on parameter-adaptive pulse-coupled neural network and convolutional sparse representation. Comput Math Methods Med 2020; 2020: 3290136. http://dx.doi.org/10.1155/2020/3290136 PMID: 32411280

[100] Padmavathi K, Asha CS, Maya VK. A novel medical image fusion by combining TV-L1 decomposed textures based on adaptive weighting scheme. Eng Sci Technol 2020; 23(1): 225-39.

[101] Liu Y, Chen X, Ward RK, Wang ZJ. Medical image fusion *via* convolutional sparsity based morphological component analysis. IEEE Signal Process Lett 2019; 26(3): 485-9. http://dx.doi.org/10.1109/LSP.2019.2895749

[102] Kaur K, Budhiraja S, Sharma N. Multimodal Medical Image Fusion based on Gray Wolf Optimization and Hilbert Transform. Biomed Pharmacol J 2019; 12(4): 2091-8. http://dx.doi.org/10.13005/bpj/1844

[103] Singh S, Anand RS. Multimodal medical image fusion using hybrid layer decomposition with CNN-based feature mapping and structural clustering. IEEE Trans Instrum Meas 2019; 69(6): 3855-65. http://dx.doi.org/10.1109/TIM.2019.2933341

[104] Reena Benjamin J, Jayasree T. Improved medical image fusion based on cascaded PCA and shift invariant wavelet transforms. Int J CARS 2018; 13(2): 229-40. http://dx.doi.org/10.1007/s11548-017-1692-4 PMID: 29250750

[105] Yadav SP, Yadav S. Image fusion using hybrid methods in multimodality medical images. Med Biol Eng Comput 2020; 58(4): 669-87. http://dx.doi.org/10.1007/s11517-020-02136-6 PMID: 31993885

[106] Jany Shabu SL, Jayakumar C. Detection of brain tumour by image fusion using SVM classifier. Comput Eng Intell Sys 2017; 8(7): 18-22.

[107] Saboori A, Birjandtalab J. PET–MRI image fusion using adaptive filter based on spectral and spatial discrepancy. Signal Image Video Process 2019; 13(1): 135-43. http://dx.doi.org/10.1007/s11760-018-1338-1

[108] Li Y, Jiang Y, Gao L, Fan Y. Fast mutual modulation fusion for multi-sensor images. Optik (Stuttg) 2015; 126(1): 107-11. http://dx.doi.org/10.1016/j.ijleo.2014.08.136

[109] Xu Z. Medical image fusion using multi-level local extrema. Inf Fusion 2014; 19: 38-48. http://dx.doi.org/10.1016/j.inffus.2013.01.001

[110] Liu Z, Song Y, Sheng VS, *et al.* MRI and PET image fusion using the nonparametric density model and the theory of variable-weight. Comput Methods Programs Biomed 2019; 175: 73-82. http://dx.doi.org/10.1016/j.cmpb.2019.04.010 PMID: 31104716

[111] Lu H, Zhang L, Serikawa S. Maximum local energy: An effective approach for multisensor image fusion in beyond wavelet transform domain. Comput Math Appl 2012; 64(5): 996-1003. http://dx.doi.org/10.1016/j.camwa.2012.03.017

[112] Li X, Zhang X, Ding M. A sum-modified-Laplacian and sparse representation based multimodal medical image fusion in Laplacian pyramid domain. Med Biol Eng Comput 2019; 57(10): 2265-75. http://dx.doi.org/10.1007/s11517-019-02023-9 PMID: 31410692

[113] Aishwarya N, Bennila Thangammal C. A novel multimodal medical image fusion using sparse representation and modified spatial frequency. Int J Imaging Syst Technol 2018; 28(3): 175-85. http://dx.doi.org/10.1002/ima.22268

[114] Liu D, Chen X, Peng D. Cosine similarity measure between hybrid intuitionistic fuzzy sets and its application in medical diagnosis. Comput Math Methods Med 2018; 2018: 3146873. http://dx.doi.org/10.1155/2018/3146873 PMID: 30416537

[115] Gambhir D, Manchanda M. A novel fusion rule for medical image fusion in complex wavelet transform domain. Int J Image Graph 2016; 16(04): 1650022. http://dx.doi.org/10.1142/S0219467816500224

[116] Yang Y, Tong S, Huang S, Lin P. Dual-tree complex wavelet transform and image block residual-based multi-focus image fusion in visual sensor networks. Sensors (Basel) 2014; 14(12): 22408-30. http://dx.doi.org/10.3390/s141222408 PMID: 25587878

[117] XZheng Y, Blasch E, Liu Z. Multispectral image fusion and colorization. Bellingham, Washington: SPIE Press 2018; pp. 230-2.

[118] Zhang L, Zhang L, Mou X, Zhang D. FSIM: A feature similarity index for image quality assessment. IEEE Trans Image Process 2011; 20(8): 2378-86. http://dx.doi.org/10.1109/TIP.2011.2109730 PMID: 21292594

[119] Zhan K, Li Q, Teng J, Wang M, Shi J. Multifocus image fusion using phase congruency. J Electron Imaging 2015; 24(3): 033014. http://dx.doi.org/10.1117/1.JEI.24.3.033014

[120] Naidu VP, Raol JR. Pixel-level image fusion using wavelets and principal component analysis. Def Sci J 2008; 58(3): 338. http://dx.doi.org/10.14429/dsj.58.1653

[121] Al-Wassai FA, Kalyankar NV, Al-Zaky AA. Studying satellite image quality based on the fusion techniques. arXiv 2011; 2011: 1110.4970.

[122] Mhangara P, Mapurisa W, Mudau N. Comparison of image fusion techniques using satellite pour l'Observation de la Terre (SPOT) 6 satellite imagery. Appl Sci (Basel) 2020; 10(5): 1881. http://dx.doi.org/10.3390/app10051881

[123] Memon F, Unar MA, Memon S. Image quality assessment for performance evaluation of focus measure operators. Mehran Univ Res J Eng Technol 2015; 34(4): 379-86.

[124] Thakur KV, Damodare OH, Sapkal AM. Identification of suited quality metrics for natural and medical images. Signal Image Process. Int J 2016; 7(3): 29-43.

[125] Singh R, Khare A. Fusion of multimodal medical images using Daubechies complex wavelet transform–A multiresolution approach. Inf Fusion 2014; 19: 49-60. http://dx.doi.org/10.1016/j.inffus.2012.09.005

[126] Dammavalam SR, Maddala S, Prasad MH. Quality assessment of pixel-level imagefusion using fuzzy logic. Int J Soft Comput 2013; 3(1): 13-25.

[127] Pistonesi S, Martinez J, Ojeda SM, Vallejos R. Structural similarity metrics for quality image fusion assessment: Algorithms. Image Process On Line 2018; 8: 345-68. http://dx.doi.org/10.5201/ipol.2018.196

[128] Aslantas V, Bendes E. A new image quality metric for image fusion: The sum of the correlations of differences. AEU Int J Electron Commun 2015; 69(12): 1890-6. http://dx.doi.org/10.1016/j.aeue.2015.09.004

[129] Yang Y, Zheng W, Huang S. Effective multifocus image fusion based on HVS and BP neural network. Sci World J 2014; 2014: 281073. http://dx.doi.org/10.1155/2014/281073 PMID: 24683327